THE Journal OF THE AMERICAN LEATHER CHEMISTS ASSOCIATION

February 2022 Vol. CXVII, No.2 *JALCA* 117(2), 45–84, 2022

116th Annual Convention

to be held at the
Eaglewood Resort & Spa
1401 Nordic Road
Itasca, IL 60143

DATE CHANGE:
June 21-24, 2022

For more information go to:
leatherchemists.org/
annual_convention.asp

Contents

Distributed by
University of CINCINNATI
LIBRARY PUBLISHING SERVICES

An imprint of the University of Cincinnati Press

ISSN: 0002-9726

Communications for Journal Publication

Manuscripts, Technical Notes and Trade News Releases should contact:
Mr. Steven D. Lange, Journal Editor, 1314 50th Street, Suite 103, Lubbock, TX 79412, USA
E-mail: jalcaeditor@gmail.com Mobile phone: (814) 414-5689

Contributors should consult the Journal Publication Policy at:
http://www.leatherchemists.org/journal_publication_policy.asp

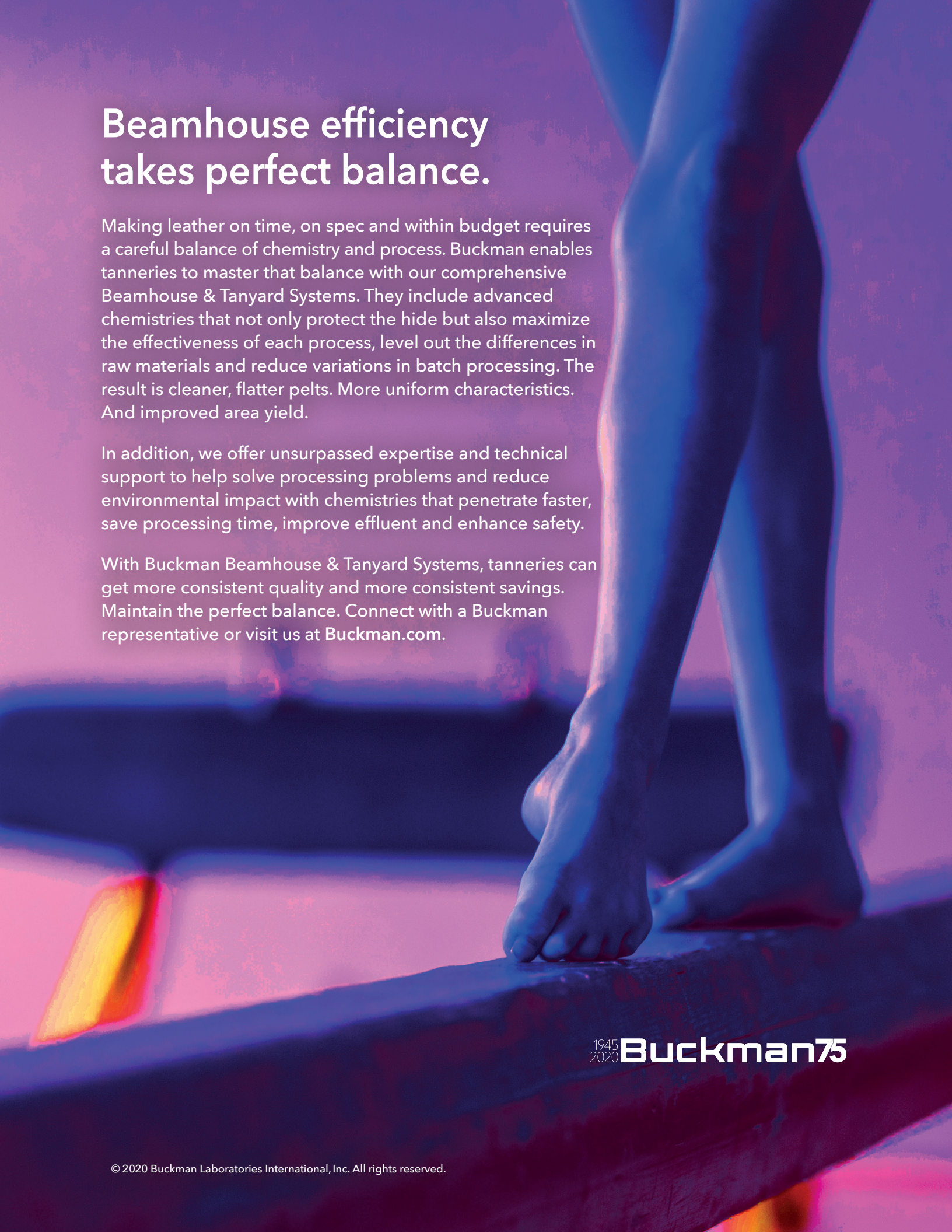

Beamhouse efficiency takes perfect balance.

Making leather on time, on spec and within budget requires a careful balance of chemistry and process. Buckman enables tanneries to master that balance with our comprehensive Beamhouse & Tanyard Systems. They include advanced chemistries that not only protect the hide but also maximize the effectiveness of each process, level out the differences in raw materials and reduce variations in batch processing. The result is cleaner, flatter pelts. More uniform characteristics. And improved area yield.

In addition, we offer unsurpassed expertise and technical support to help solve processing problems and reduce environmental impact with chemistries that penetrate faster, save processing time, improve effluent and enhance safety.

With Buckman Beamhouse & Tanyard Systems, tanneries can get more consistent quality and more consistent savings. Maintain the perfect balance. Connect with a Buckman representative or visit us at **Buckman.com**.

1945 2020 Buckman75

JOURNAL OF THE
AMERICAN LEATHER CHEMISTS ASSOCIATION

Proceedings, Reports, Notices, and News
of the
AMERICAN LEATHER CHEMISTS ASSOCIATION

THE JOURNAL OF THE AMERICAN LEATHER CHEMISTS ASSOCIATION (USPS #019-334) is published monthly by The American Leather Chemists Association, 1314 50th Street, Suite 103, Lubbock, Texas 79412. Telephone (806)744-1798 Fax (806)744-1785. Single copy price: $8.50 members, $17.00 non-member. Subscriptions: $185 for hard copy plus postage and handling of $60 for domestic subscribers and $70 for foreign subscribers; $185 for ezine only; and $205 for hard copy and ezine plus postage and handling of $60 for domestic subscribers and $70 for foreign subscribers.

Periodical Postage paid at Lubbock, Texas and additional mailing offices. Postmaster send change of addresses to The American Leather Chemists Association, 1314 50th Street, Suite 103, Lubbock, Texas 79412.

Website: www.leatherchemists.org E-mail: carol.adcock@ttu.edu

COLD
Milling

Smooth Leather Milling

Erretre
Tannery Innovations

Erretre s.p.a. | Via Ferraretta,1 | Arzignano (VI) 36071 | tel. +39 0444 478312 | info@erretre.com

Salt Free Preservation of Raw Goat Skin Using Swietenia Mahogany (Seed) Extract

by
Md. Abdur Razzaq,* Murshid Jaman Chowdhury and Md. Tushar Uddin
Leather Research Institute (LRI)
Bangladesh Council of Scientific and Industrial Research (BCSIR)
Nayarhat, Savar, Dhaka-1350, Bangladesh

Abstract

Curing of hides and skins using sodium salt is a well-established and economical preservation technique worldwide. But it contributes to generating a large amount of total dissolved solids (TDS) and increasing the salinity of water during leather processing which is a threat to the environment. The current research is an attempt to preserve goat skin using mahogany (*Swietenia mahogany*) seed's extract. In real practice different percentages of mahogany seed extract were applied on raw goat skin and 3% (by weight of skin) of it showed best result. To evaluate the preservation efficiency, related parameters of preservation viz. odor, hair slip, shrinkage temperature, moisture content, bacterial count etc. were monitored regularly for 30 days. The obtained results were compared with conventional salt curing process. The experimental trial showed efficiency in lessening TDS value and chloride content. The preserved goat skins of both trials were treated following conventional leather processing techniques and physical properties were studied. The discussed preservation method exhibited comparable result in every index.

Introduction

Curing is a short-term preservation technique to store and transport raw hides and skins safely for forthcoming processing operations. It is a reversible process with the objective to restore the hides and skins to the original raw condition.[1] It is essential to subject raw hides and skins to any preservation technique within 5–6 hrs after the death of the animal or flaying the skin to prevent degradation.[2] Bacteria may attack the flesh surface of hides and skins within 8–12 hours of flaying and may also form serious grain peeling and voids within 15–24 hrs.[3]

Almost 40-50% common salt (based on the green weight of skin) is applied in the curing operation which dehydrates the skin leading to hindering bacterial putrefaction.[4] The salt is discharged in the environment contributing in 70% of Total Dissolved Solids (TDS) generation during leather manufacturing.[5] Researchers around the world are in continuous effort to determine a convenient and environmentally friendly curing technique. Mentionable alternative techniques are sun drying, controlled drying, cooling and chilling, vacuum, dry ice, aryl alcohols, sodium silico-fluoride, and sulphites.[6-13] Notable chemical preservation methods are potassium chloride, boric acid, soda ash, benzalkonium chloride, antibiotics, bacteriocin, formaldehyde, silica gel, Vantocil IB, chlorites and hypochlorites, sulphates, and bisulphite-acetic acid.[14-24] None of these are accepted and practiced commercially due to potential hazards or economical non-viability.

Swietenia mahogany, a locally available, large, deciduous and economically beneficial timber tree, is commonly known as "Mahogany tree".[25] It is under the family Meliaceae and the super family swietenioideae. It is vastly available in Bangladesh as well as India, China, Africa and different parts of North and South American countries.[26] Various parts of the Mahogany viz. root, bark, seed etc. are used for the treatment of hypertension, diabetes, malaria, amoebiasis, coughs, chest pain and tuberculosis, and as an abortifacient, antiseptic, astringent, depurative, and tonic.[27] S. Mahogany seed extract can now be applied in the agricultural field to control pesticides.[28-30] Mahogany seed extract holds fatty acids like linoleic, oleic, stearic and palmitic which show activity against microorganisms.[31,32] The mahogany (Meliaceae) family is characterized by synthesis of modified triterpenes known as limonoids having a 4,4,8-trimethyl-17-furanyl steroid skeleton.

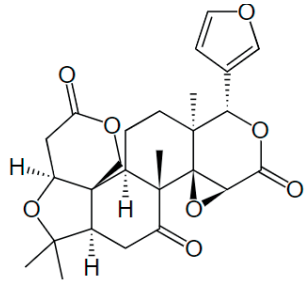

Triterpenoids present in mahogany family are an important group of constitutive defense substances against microbes.[33] Many papers have reported about the antimicrobial properties of Swietenia Mahogany seed extract.[32-38] Fresh hides and skins are attacked by bacteria like Bacillus subtilis, Escherichia coli, Micrococcus spp., Proteus vulgaris and Pseudomonas aeruginosa.[39] Sweitenia Mahogani seed extract shows antibacterial property against Bacillus Subtilis, Escherichia Coli, S. Aurous, S. typhimurium, P. aeruginosa etc. with strong inhibition zones.[26, 32] That is why it was estimated that it might be effective for the preservation of raw skin.

*Corresponding author email: arazzaq-lri@bcsir.gov.bd
Manuscript received July 23, 2021, accepted for publication September 5, 2021.

Material and Method

Collection of Skin

Freshly flayed goat skins were purchased from a local hides and skin trader in Dhamrai, Dhaka, Bangladesh. Then the skins were washed with water to remove dirt, filth, blood etc. impurities. Finally, the skins were hanged for few minutes to exude water.

Chemicals

Chemicals and auxiliaries used in the control preservation, beamhouse and post tanning operations were of commercial grade. For biochemical and pollution index determination, analytical grade chemicals were used.

Collection and Extraction of Mahogany seed

Seeds were collected from the garden of Leather Research Institute; shells were peeled and sun dried. The collected seeds were cleaned by washing with running tap water followed by drying in the sun. Then seeds were crushed into fine powder using an analytical grinder. The fine powder was extracted in a Soxhlet apparatus with methanol for 8 hours. Then the solvent was evaporated by employing a rotary evaporator at 40°C. The oily extract was then stored in a refrigerator at 4°C.

FTIR Analysis

To find out the functional group of the mahogany seed extract a Perkin-Elmer FTIR spectrophotometer with UATR was used. The absorbance, FT-IR Spectra of the samples was recorded. The FT-IR was first calibrated for background scanning signal against a control sample of pure KBr.

Application of Extract for Curing

To find out the optimum percentage of extract required for the preservation an initial trial was conducted. Two freshly flayed goat skins were made half to get four samples. Variable percentages (w/w) of extract were applied on the raw goat skin to find out the optimum percentage. The physical changes e.g., odor, hair slip, and moisture content were assessed periodically (fresh, 1st, 4th, 7th, 15th, and 30th days of preservation) and the optimum percentage was found to be 3% (w/w). During our final trial, one piece goat skin was made half to get two samples. One half was for the control trial and 50% (w/w) common salt was applied. Then the skin was kept for preservation. For the experimental trial 3% (w/w) extract was pasted on the flesh side of the other half and kept for preservation without folding. Both samples were kept in the same environmental conditions and temperature. The preservation parameters viz. moisture content (%), hair slip, odor, bacterial count, shrinkage temperature and extractable nitrogen were assessed periodically (raw, 1st, 4th, 7th, 15th and 30th days of preservation.

Moisture Content

Small pieces (1-2g) of skin samples were cut and the moisture content was determined using a High-performance Moisture Analyzer model WBA-110M.

Nitrogen Content

To determine nitrogen content a known weight (5g) from the preserved samples was taken and treated with ten times (w/v) its weight of distilled water into a conical flask. The flask was shaken at 200 rpm for 30 minutes by keeping it on a shaker. Then the liquor was filtered through a filter paper and transferred to the digestion unit of an automated Kjeldahl chamber. The nitrogen content was determined following the method described in the literature.[40]

Bacterial Count

During different stages of preservation skin samples of known weight (5g) were cut and followed the procedure of nitrogen content determination up to filtration. 1 ml of the filtrate was taken and diluted to 10 ml with sterile water. The solution was shaken well to get identical suspension of bacteria and 0.1 ml was taken in a sterile petri plate. Then, molten nutrient agar was added and shaken carefully for identical distribution of bacteria. Finally, petri plates were kept for 48 hours at 37°C in an incubator.[41]The bacterial population was counted using a bacterial colony counter.

Hydrothermal Property

Shrinkage temperature indicates the hydrothermal property of hides and skins. It was determined by using SATRA STD 114 shrinkage temperature tester.[42] Test samples (20×3 mm) were cut and hooked in the holder of the shrinkage temperature apparatus which was then immersed in a bath containing a glycerin/water solution in the ratio of 70:30. The temperature was gradually increased with the rate of the heat increase. The shrinkage starting temperature was noted as the shrinkage temperature of that particular skin.

Leather Making

The skins that were preserved for 30 days were processed up to crust leather by following conventional leather processing method.

Pollution Load Analysis

The wastewater in the soaking operation generated from the control as well as experimental trial was collected and analyzed for biochemical oxygen demand (BOD), chemical oxygen demand (COD), total dissolved solids (TDS) and chloride content. The standard APHA methods were followed in analysis and all the experiments were triplicated.[43]

Physical Properties Analysis

The prepared crust leathers were left about 1 month for aging. Physical strength of the leathers was determined after conditioning at temperature 23 ± 2°C and relative humidity 65 ± 2% for 48 hours. Then the samples were taken from the specified sampling location.

The properties such as the tensile strength, elongation at break, tear strength, and bursting strength were assessed following SATRA TM 43, TM 162, and TM 24 respectively.

SEM Analysis

To evaluate the morphological characteristics of crust leathers from the preserved control and experimental goat skins samples from each were subjected to JEOL Field Emission Scanning Electron Microscope (JSM-7610F, Japan). The photographs of the grain surface were taken at an accelerating voltage 15.0 kV with magnification 40X. The fiber images (flesh side) were assessed by accelerating voltage 15.0 kV with magnification 1000X.

Results and Discussion

Organoleptic Properties

Organoleptic properties of the preserved skins were assessed periodically from the zero (0) day to the 30th day of preservation.

Table I

Organoleptic Properties of goat skin preserved with mahogany seed extract

Day	Hair slip	Odor	Physical feel
0	No	No	Soft
1	No	No	Soft
3	No	No	Medium hard
6	No	No	Medium hard
12	No	No	Medium hard
18	No	No	Medium hard
24	No	No	Medium hard
30	No	No	Medium hard

Hair slip, odor and physical feel are common organoleptic properties of skin preservation. Those properties are illustrated in the Table I. There was no hair slip during the whole preservation period. The skin gradually became hard and reached a medium hardness at the 3rd day of preservation. No bad odor was generated. This indicates that neither significant bacterial growth nor putrefaction occurred.

FTIR Analysis

Based on the IR spectrum of mahogany seeds extract, it was seen that the sharp peak at 2923.08 cm-1 showed the presence of -CH and 2853.71 cm-1 with a range of -CH_2, and at 1377.88 cm-1 showed the presence of -CH_3 group. Absorption band at 1458.26 cm-1 is for N-O stretching and shows the presence of nitro compound. The peak at1181.15 cm-1 stands for C-O stretching and identifies tertiary alcohol. The spectrum at 1743.65 cm^{-1} shows the C=O stretching and proved the presence of ester which proves antimicrobial possibility of mahogany seed extract.[44]

Moisture Content

The moisture content is one of the important parameters to assess the effectiveness of a curing agent. The analysis of the moisture content of both trials is displayed in Table II covering the whole preservation of 30 days. Gradual decreases of moisture with the increase of preservation time have been depicted in Table II. The moisture content of control trial decreases gradually and ends at 35% after the preservation period. On the other hand, moisture content of experimental trial decreases to 40% within preservation period of a single day. The final moisture content of the experimental was found 19% after 30 days preservation. It indicates that the experimental trial dehydrates the sample more than the control trial. The greater reduction in moisture content might be due to that the skin's water gradually evaporates by atmospheric action since fatty acids of mahogany seed extract react a little with water.[45] In case of the control trial, hydrolysis reaction occurred and a mentionable amount of water prevails on the surface of skin.

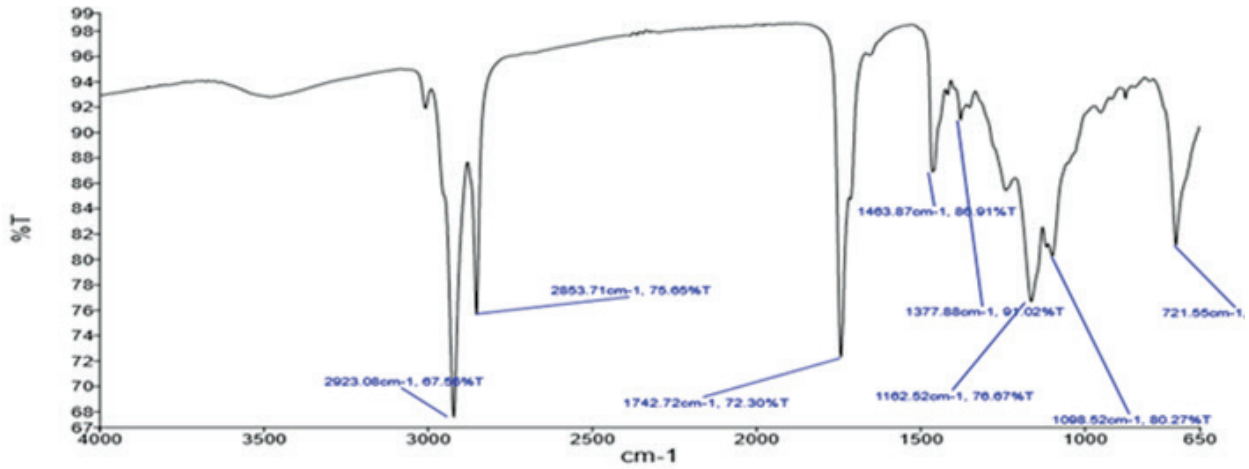

Figure 1. FTIR Spectrum of mahogany seed extract.

Table II

Moisture Content (%) of preserved skins

Day	Experimental (Mahogany seed extract based preservation, 3% of raw weight)	Control Trial (Common Salt preservation, 50% of raw weight)
0	66	66
1	40	58
4	34	55
7	30	49.4
15	20	44
30	19	35

Table III

Nitrogen Content (gm/kg of sample) of preserved skins

Day	Experimental (Salt Cured) (gm/kg)	Control trial (MSE Cured) (gm/kg)
0	1.18±0.04	1.18±0.02
1	0.3±0.03	0.6±0.02
4	0.1±0.02	0.5±0.03
7	0.05±0.01	0.1±0.03
15	0.28±0.03	0.24±0.02
30	0.37±0.02	0.28±0.01

Values are mean ± standard deviation of three determinations.

Nitrogen Content

Total extractable nitrogen for the skin preserved with experimental and control trial has been illustrated in Table III. Gradual decrease in total extractable nitrogen was found in control and experimental trial. The final result after the preservation period was 0.28 gm/kg and 0.37gm/kg for control and experimental trial respectively. This might be due to the antimicrobial activity of the preservatives, thus inhibiting putrefaction.

Bacterial Count

The bacterial count in the preserved skins is depicted in Table IV. In raw goat skin bacterial count was 3×10^3 CFU/g. The bacterial count of the experimental trial was 4×10^3 after day 1 whereas it was 2×10^8 in the control trial. The drastic reduction in bacterial count at the experimental trial might be due to reduced moisture and nitrogen content. The bacterial count of both trials showed steadiness during the 30 days preservation period. The bacterial counts of experimental and control trial were 1×10^4 and 6×10^8 respectively. The increase of bacteria in the experimental trial might be due to the increase of nitrogen content. Literature shows inhibition of mahogany seed extract against various microbes. Amongst various microbes the Bacillus Subtilis was inhibited strongly. [26, 32]

Shrinkage temperature

Hydrothermal stability (Shrinkage temperature) is another important indicator of stability of leather and is reported in Table V. The initial shrinkage temperature was 66°C. Although the shrinkage temperature of the experimental trial was found to slightly decrease after 1 day preservation period, it started to increase slowly. On the other hand, the control trial exhibited a gradual decrease and the final shrinkage temperature was 62°C whereas, the final shrinkage temperature of the experimental trial was 73°C. Literature shows the presence of tannins and phenolic compounds in swietenia mahagoni.[46] Thus, elevation in shrinkage temperature of experimental trial might be due to the tanning effect of the seed extract.

Pollution load Analysis

The pollution load status of the experiment has been depicted in Table VI. There is little change in the BOD and COD levels, but significant reduction in TDS and Chloride content in the experimental trial. Since there was no use of salt, chloride content is completely reduced. Besides, the value of total dissolved solid (TDS) was significantly reduced to 97%.

Table IV

Bacterial Count in the preserved skins

Day	Experimental (CFU/g)	Control (CFU/g)
0	3×10^3	3×10^3
1	4×10^3	2×10^8
4	5×10^3	6×10^9
7	2×10^4	5×10^9
15	3×10^4	3×10^7
30	1×10^4	6×10^8

Table V

Shrinkage Temperature (°C) of Preserved Skins

Day	Experimental (°C)	Control (°C)
0	66±1	66±1
1	64.2±1	65.5±2
4	68±1	63±1
7	66.5±2	62±1
15	68±2	61±2
30	73±1	62±1

Values are mean ± standard deviation of three determinations.

Table VI

Pollution Load Status of soaking liquor

Pollution Parameter	Experimental (mg/L)	Control (mg/L)
BOD	1012	1178
COD	2120	4166
TDS	525	18000
Cl	36	11768

Physical properties study

Physical strength evaluation of the crust upper leather of experimental in comparison with the control has been done. The crust leathers were assessed for softness, grain tightness, fullness, and smoothness. The tabulated physical properties in Table VII indicate that the physical strength values e.g., tensile strength, elongation at break, tear strength and grain crack of the experimental skin preserved with mahogany seed extract were comparable with corresponding control method. The elongation at break (%) and load at grain crack (kg) values fulfilled the required values.

Table VII

Physical properties of processed crust leather.

Parameter	Experimental	Control
Tensile strength	29.5±0.8 N/mm^2	30±0.7 N/mm^2
Elongation at break	52.5±0.5 N	46.5±0.6 N
Tear strength	69±0.8 N	89.5±0.8 N
Ball Burst Test	71.6±0.6 N	74.5±0.6 N

Values are mean ± standard deviation of three determinations.

SEM Analysis

SEM photographs of the leather processed from the control trial and experimental trial have been illustrated. The Figure 2 shows the images of the grain side of experimental and control trials respectively. Both samples show slight flatness of the grain texture (grain side).

The Figure 3 shows the fiber pattern (flesh side) of both trials. It indicates that there are no significant change in the leather prepared from the experimental goat skin compared with the control. This proves that the texture and quality of the goat skin was almost the same using the new preservation method.

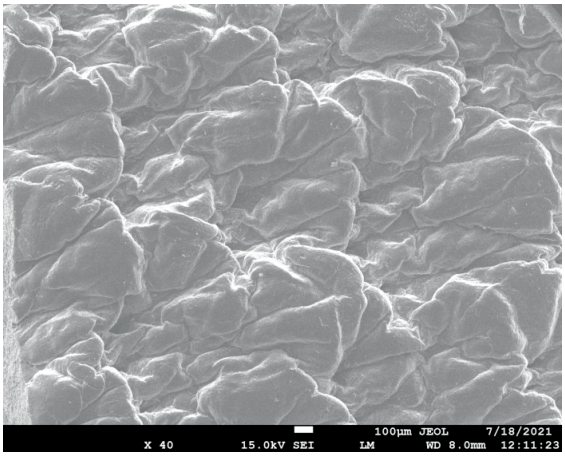

SEM image of grain pattern of experimental trial

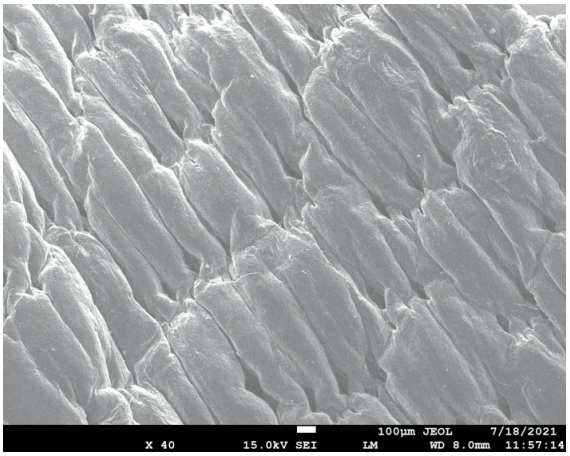

SEM image of grain pattern of control trial

Figure 2.

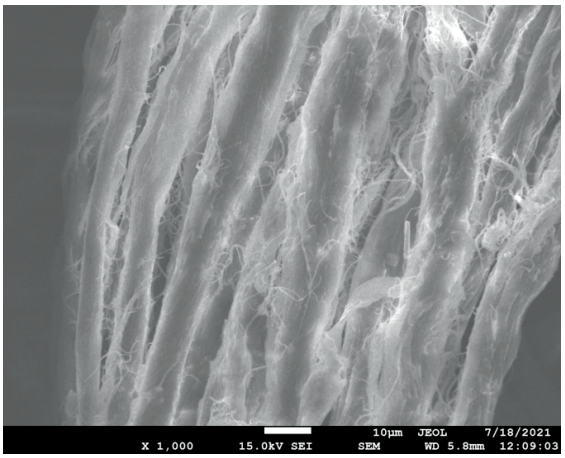

SEM image of fiber pattern (flesh side) of experimental trial

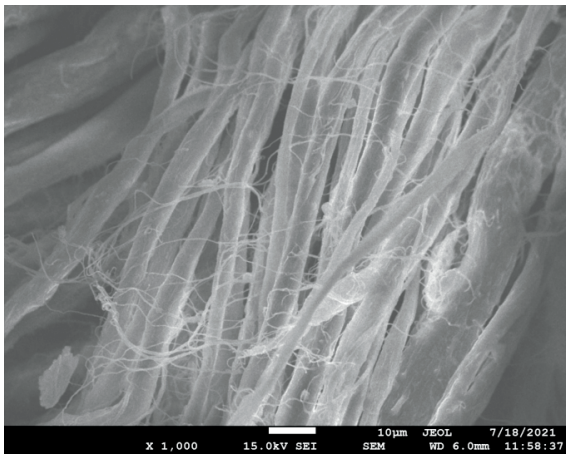

SEM image of fiber pattern (flesh side) of control trial

Figure 3.

Conclusion

Due to environmental compliance, researchers as well as factory owners are highly interested to find an alternative to salt curing. The mahogany seed extract can be an alternative way of animal skin curing. This is a salt-free curing technique which remarkably decreases the environmental pollution load in every index. In addition to that, the experimental curing technique can preserve skin for more than one month. Thus, it is expected to be one of the more viable curing techniques for preservation of skins in the leather industry.

Acknowledgement

Authors wish to thank the personnel who helped to conduct this research at the Leather Research Institute (LRI). Authors also convey special gratitude to the director of LRI and Chairman of Bangladesh Council of Scientific and Industrial Research (BCSIR) for aiding in every step of compliance and funding.

References

1. Hashema, M.A., Hasan, M., Momen, M. A., Payel, S.; Minus Salt Goat Skin Preservation: Extreme Chloride Reduction In Tannery Wastewater, XXXV Congress of IULTCS, 2019.
2. Kanagaraj, J., Sundar, V. J., Muralidharan, C., Sadulla, S.; Alternatives to sodium chloride in prevention of skin protein degradation- A case study. *J. Clean. Prod.* 13, 825–831, 2005.
3. Aslan, E., Birbir, M.; Examination of gram-positive bacteria on salt-pack cured hides. *JALCA* 106, 372–380, 2011.
4. Hashem, M.A., Arman, M.N., Sheikh. M.H.R. and Islam. M.H.; Sodium Chloride Substitute for Lower Salt Goat Skin Preservation: A Novel Approach, *JALCA* 112, 270-276, 2017
5. Kanagaraj, J., Sastry, T.P. and Rose, C.; Effective preservation of raw goat skins for the reduction of total dissolved solids, *J. of Clean. Prod*. 13, 959-964, 2004.
6. Roddy W. T., Hermoso R. P.; The coagulable protein of animal skin, *JALCA* 38, 96, 1943
7. Waters P. J., Stephen L. J., Sunridge; Controlled drying, *JSLTC* , 65, 41, 1981
8. Babu N. K. C., Karthikeyan R., Swarna B., Ramesh R., Shanthi C., Sadulla S.; A systematic study on the role of chilling temperatures on the curing efficacy of hides and skins, *JALCA* 107(11), 362–370, 2012
9. Gudro I., Valeika V., Sirvaityte J.; Short Term Preservation of Hide Using Vacuum, *PLOS ONE,* 9(11), 1-9, 2014
10. Sathish M., Madhan B., Saravanan P., Rao J. R., Nair B. U.; Dry ice - an eco-friendly alternative for ammonium reduction in leather manufacturing, *J. Clean. Prod*., 54, 289-295, 2013
11. Venkatachalam P., Sadulla S., Duraiswamy B.; Further experiments in salt-less curing *Leather Science*, 29, 217221, 1982
12. Haines; Short term preservation with various preservatives, *JALCA*, 57, 356, 1973
13. Vankar P. S., Dwovedi A. K.; Sulphates for skin preservation-A novel approach to reduce tannery effluent salinity hazards, *J Hazard Mater*, 163(1): 207-212, 2009
14. Bailey, D. G., Gosselin, J. A.; The preservation of animal hides and skins with potassium chloride. *JALCA* 91, 317– 333, 1996.
15. Hughes, I. R.; Temporary preservation of hides using boric acid. *JSLTC* 58, 100–103, 1974.
16. Rao, B. R., Henrickson, R. L.; Preservation of hides with soda ash. *JALCA* 78, 48–53, 1983.
17. Cordon, T. C., Jones, H. W., Naghski, J., Jiffee, J. W.; Benzalkonium chloride as a preservative for hide and skin. *JSLTC,* 59, 317–326, 1964.
18. Berwick, P. G., Gerbi, S. A., Russel, A. E.; Antibiotics to control green hide biodeterioration for short term preservation. *JSLTC*, 74, 151, 1996.
19. Kanagaraj, J., Tamil Selvi, A., Senthilvelan, T., Chandra Babu, N. K., Chandrasekar, B.; Evaluation of new bacteriocin as a potential short-term preservative for goat skin. *AJMR* 2, 86–93, 2014.
20. Sharphouse, J., H, Kinweri, G.; Preservation-formaldehyde, of raw hides and skins. *JSLTC,* 62, 119–23, 1978.
21. Kanagaraj, J., Chandra Babu, N. K., Sadulla, S., Rajkumar, G. S., Visalakshi, V., Chandra Kumar, N.; Cleaner techniques for the preservation of raw goat skins. *J. Clean. Prod*. 9, 261– 268, 2001.
22. Haines, B. M.; The temporary preservation of sheep skins: Trials with Vantocil IB. *JSLTC*, 57, 84–92, 1973.
23. Margold, F., Heidemann, E.; Short-term preservation with less salt method. *Leder* 29, 65–80, 1977.
24. Hopkins, W. J., Bailey, D. G., Seigler, M.; Tannery scale evaluation of hide preservation by sulphite-acetic acid applied in a drum and a hide processor. *JALCA* 76, 134–139, 1981.
25. Sahgal, G.,Ramanathan, S., Sasidharan, S., Mordi, M.N., Ismail, S.,Mansor, S.M.; Phytochemical and antimicrobial activity of Swieteniamahagoni crude methanolic seed extract, *Tropical Biomedicine*, 26(3), 274–279 (2009)
26. Alam, M. K., Mansur, F.J., Karim, M. M., Haque, M. A.; Antimicrobial Activity Of Swietenia Mahagoni (Seed) Against Various Pathogenic Microbes, *Indo American Journal Of Pharmaceutical Research*, 4(05), 2362-2366, 2014.
27. Rahman A.K.M.S., Chowdhury, A.K.A., Husne-Ara, A., Sheikh Z.R., Mohammad S.A., Lutfun, N., Satyajit S.D.; Antibacterial Activity of Two Limonoids from Swietenia Mahagoni against Multiple-Drug-Resistant (MDR) Bacterial Strains, *J. Nat. Med.* , 63, 41-45, 2009.
28. Bamaiyi, L. J., Iliya S. Ndams, I. S., Toro, W. A., Odekina, S.; Effect of Mahogany Khayasenegalensis Seed Oil in the Control of Callosobruchusmaculatus on Stored Cowpea, Plant Protect. *Sci*, 42(4) 130–134, 2006.
29. Parvin, S., Zeng, X., Islam, T.; Bioactivity of Indonesian mahogany, Toonasureni (Blume) (Meliaceae), against the red flour beetle, Triboliumcastaneum (Coleoptera, Tenebrionidae); *Revista Brasileira de Entomologia*, 56(3), 354–358, 2012
30. Mivanyi, R., Adamu, M., hingu, D.; The Toxicity of Mahogany Seed Oil Against Callosobruchus Maculates in Storage of Cowpea (Vigna Unguiculata) in Hong District Adamawa State. Nigeria,

American Journal of Engineering Research (AJER), 6(12), 63-66, 2017.

31. Huang C. B., George B., Ebersole J. L.; Antimicrobial activity of n-6, n-7 and n-9 fatty acids and their esters for oral microorganisms, *Archives of Oral Biology*, 55(8), 555-560, 2010.
32. Suliman, M. B., Nour, A.H., Yusoff, M.M., Nour, A. H., Kuppusamy, P., Yuvaraj, A. R., Adam, M. S.; Fatty acid composition and antibacterial activity of Swietenia Macrophylla king seed oil, *African Journal of Plant Science*, 7(7), 300-303, 2013.
33. Paritalaa,V., Chiruvellab, K. K., Thamminenic,C., Ghantad, R. G., Mohammed, A.; Phytochemicals and antimicrobial potentials of mahogany family, *Revista Brasileira de Farmacognosia* 25, 61–83, 2015.
34. Durai, M.V., Balamuniappan,G.,Geetha, S.; Phytochemical screening and antimicrobial activity of leaf, seed and central-fruit-axis crude extract of Swietenia macrophylla King, *JPP* 5(3), 181-186, 2016
35. Ali, M.A., Sayeed, M.A., Islam, M.S., Yeasmin, M.S., Khan,G.R.M.A.M., Muhamad. I. I.; Physicochemical and Antimicrobial Properties of Trichosanthes Anguina and Swietenia Mahagoni Seeds, *Bull. Chem. Soc. Ethiop*., 25(3), 427-436, 2011.
36. Mohammed, S. B., Azhari, N. H., Mashitah, Y. M., Abdurahman, N. H., Mazza. A. S.; Physicochemical Characterization and Antimicrobial Activity of Swietenia Macrophylla King Seed Oil, *IJERT*, 3(3), 2014.
37. Nour, A. H., Nour, A. H., Sandanasamy, J. A/P., Yusoff. M. M.; Antibacterial Activity of Different Extracts of Swietenia Macrophylla King, 13th Medicinal and Aromatic Plants Seminar 2012 (MAPS2012), 25-26, 2012.
38. Sundar, D. S., Anandan, S., Namasivayam, S. K. R.; Antifungal activity of Swietenia mahogany on Candida albicans and Cryptococcus neoformans, *J. Microbiology and Antimicrobials,* 5(6), 55-59,2013.
39. Fontoura, J.T., Ody D., Gutterres M.; Performance of Antimicrobial Agents for the Preservation of Chrome Leather, *JALCA* 111, 221-229, 2016.
40. Bureau of Indian Standards, Chemical testing of leather, 1971.
41. R. Cruickshank, Determination of bacterial count method, medical microbiology, 768–769, 1965.
42. SLTC Official Methods of Analysis, 1996.
43. APHA, Standard Methods for the Examination of Water and Wastewater, American Public Health Association, American Water Works Association, Water Environment Federation, Washington DC. 2012
44. Silva, R. H. N., Andrade A. C. M., Nóbrega D. F., Castro R. D., Pessôa H. F., Rani N., Sousa D. P.; Antimicrobial Activity of 4-Chlorocinnamic Acid Derivatives, *BioMed Research International,* 1-13, 2019.
45. Thomas E.; Lipid, Encyclopedia Britannica, 2020.
46. Hajra S. , Mehta A.; Phenolic compounds and antioxidant activity of swietenia mahagoni seeds, *International Journal of Pharmacy and Pharmaceutical Sciences*, 3,431-434,2011.

Carbonization Region Measurement in Vegetable Tanned Goat Leather using Machine Vision System for Evaluating Performance Measures of Leather Cut Contour Edges

by

S. Vasanth,[1] T. Muthuramalingam,[1*] and Sanjeev Gupta[2]

Department of Mechatronics Engineering, SRM Institute of Science and Technology, Kattankulathur, India[1]

Unit for science dissemination, Central Leather Research Institute, Chennai, India[2]

Abstract

Due to the widespread application and popularity of lasers in recent times, the usage of laser cutting for leather applications has increased as well. Laser technology is needed to provide more consistent and effective results while cutting leathers that include complicated geometries particularly in several sectors where leathers are often utilized such as footwear, apparel and fashion accessories. In this investigation, the diode laser was preferred for leather cutting due to its regulated power density, compact size and portability whereas the CO_2 lasers are uncontrollable. The benefit of employing a diode laser is that it can overcome some of the disadvantages associated with CO_2 lasers such as power consumption, carbonization layer and geometric inaccuracy. There is no technique available to measure the carbonization at the leather cut contour edges. Hence an attempt has been made to investigate the carbonization percentage with the help of a machine vision system to improve the machining process. The technique of measuring carbonization can be used effectively in the leather industry for the accurate measurement of carbonization. The lower duty cycle with moderate pulse width modulation (PWM) and amplitude could produce lower carbonization layer. PWM frequency has a high influential role on determining carbonization in leather cutting.

Introduction

The advancement in the leather cutting is necessary owing to the increased usage of such materials. For cutting intricate geometries, laser cutting process is preferable as it has maximum versatility, efficient setup and high adaptability to various material characteristics. For designers, these characteristics make laser an enticing tool.[1] Diode lasers have made enormous advances in applied physics that have proven new and ground-breaking techniques to researchers. Due to their efficiency and low operating cost, diode laser systems are especially important and have emerged as preferred equipment for tackling a broad variety of material processing applications.[2] The industrial application environment is now dominated by CO_2 and fiber laser sources. Diode laser technology has improved rapidly for material processing in cutting applications. They are typically inexpensive which may be utilized to provide much more laser power in combination. The direct use of a diode beam for material processing is a new accomplishment.[3] It is important to develop diode laser technology for cutting leathers with complex geometries under improved environmental measures such as carbonization, striations and dross formation in leather cutting. The carbonization in leather cutting is reduced by the lower focused energy from a laser power diode.[4] Laser assisted oxygen cutting (LASOX) is mostly favored due to its ability of easy adaptability for cutting thick mild carbon steel.[9] The conventional lasers have certain disadvantages in terms of cutting such as geometrical inaccuracies, carbonization, overcut etc. The usage of laser diodes may help to minimize this problem. The primary reason for utilizing a laser diode is to save energy.[5] In the laser power diode based leather cutting process, standoff distance has a significant impact on defining the lowest carbonization area and kerf width. If the diode laser module is not calibrated correctly, it may result in burns and undercuts while cutting leather. Changing the focal length of the laser module improves the cutting process.[6] Productivity measurement relies on the process parameters of input and output. In order to increase the effectiveness of the system, it is extremely important to evaluate the effects of the input process parameters on response parameter.[7] The manual inspection of leather is time consuming with high risks. The usage of a commercial digital camera resulted in poor enlarged pictures, which is one of the major disadvantages. Digital microscopic leather pictures are processed digitally to examine the darkening effects due to the thermal effect of the diode laser.[8,9] The laser cutting of leather was carried out using diode laser with the wavelength of 450nm. The diode based laser beam machining (LBM) process delivers superior results than CO_2 and other manual cutting procedures.

From the detailed literature, no suitable method to measure carbonization region on leather cutting has been found so far. Hence the present investigation has been made. In the present study, an attempt has been made to utilize the camera as sensing element to measure carbonization region. The novel measurement algorithm has been proposed and explained. Hence an attempt was undertaken

*Corresponding author email: muthu1060@gmail.com

Manuscript received July 8, 2021, accepted for publication September 14, 2021.

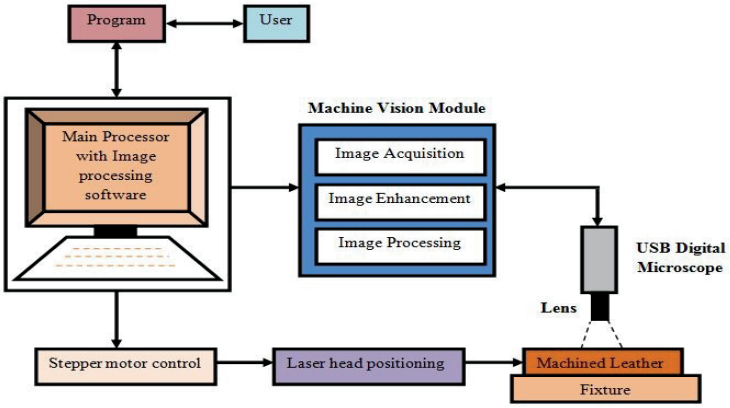

Figure 1. Machine vision based leather inspection

in this research to evaluate leather machinability and to measure carbonization region on leather cutting using a diode based laser beam machining process.

Experimental methodology

Natural vegetable tanned goat skin leather samples were utilized in the present study. The leather samples were purchased from M/s. Shafeeq Shameel & Co., Ambur, Tamilnadu, India. This leather is characterized by a particular grainy surface typical of the goat that together with a natural color and a soft temper make it the ideal material for leather goods making such as small bags, shoes, linings, wallets, crafts and bindings. Figure 1 shows human-machine interface carried out by means of the software Elekscam Evolution Desktop CAM v3.1 for laser control and MATLAB 2019a for the image analysis. The Firmwares can be readily available for converting G-codes to Embedded C and converting drawings to G-codes. The Elekscam firmware was used to control the movement of the system. The speed of the motor movement was controlled using G-codes. The input from the geometrical shape and leather cut dimension was done by means of G-codes uploading through Elekscam. Through the computer the instructions were provided for image acquisition, processing and other activities. The user controls the laser action on the leather by interfacing with the computer and also the machine vision module. The computer controls the stepper motors complete operation including displacement in the X-Y direction.

Machine vision module arrangement

Image acquisition of leather specimens

Image acquisition is the process of obtaining the image. It is acquired via the use of Celestron Handheld USB digital microscope with the 5 MP CMOS imaging Sensor and 1600 x 1200 pixel array size. Image acquisition is a critical component of image processing because it should grasp the maximum information from the outside so that it can be used for processing. The microscope was utilized in the present study to take the magnified image.

Figure 2 shows the image captured using Celestron microscope The digital microscope comes with an inbedded digital camera and software for acquiring the image. When the microscope camera is connected to a computer, its field of view is shown on the computer through software. This assists the user in capturing the desired field of area.

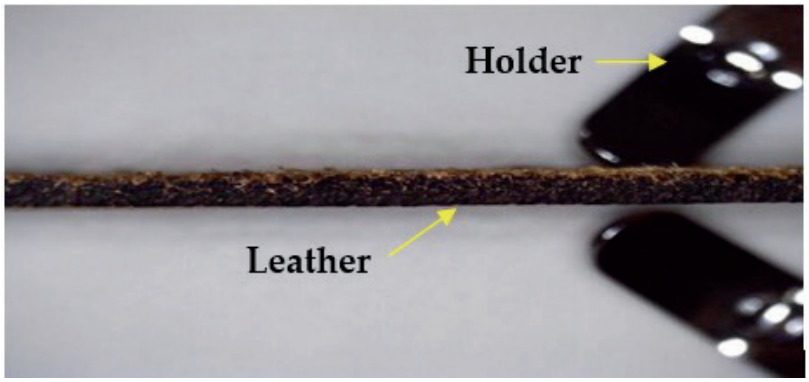

Figure 2. Leather cross section captured using Celestron digital microscope

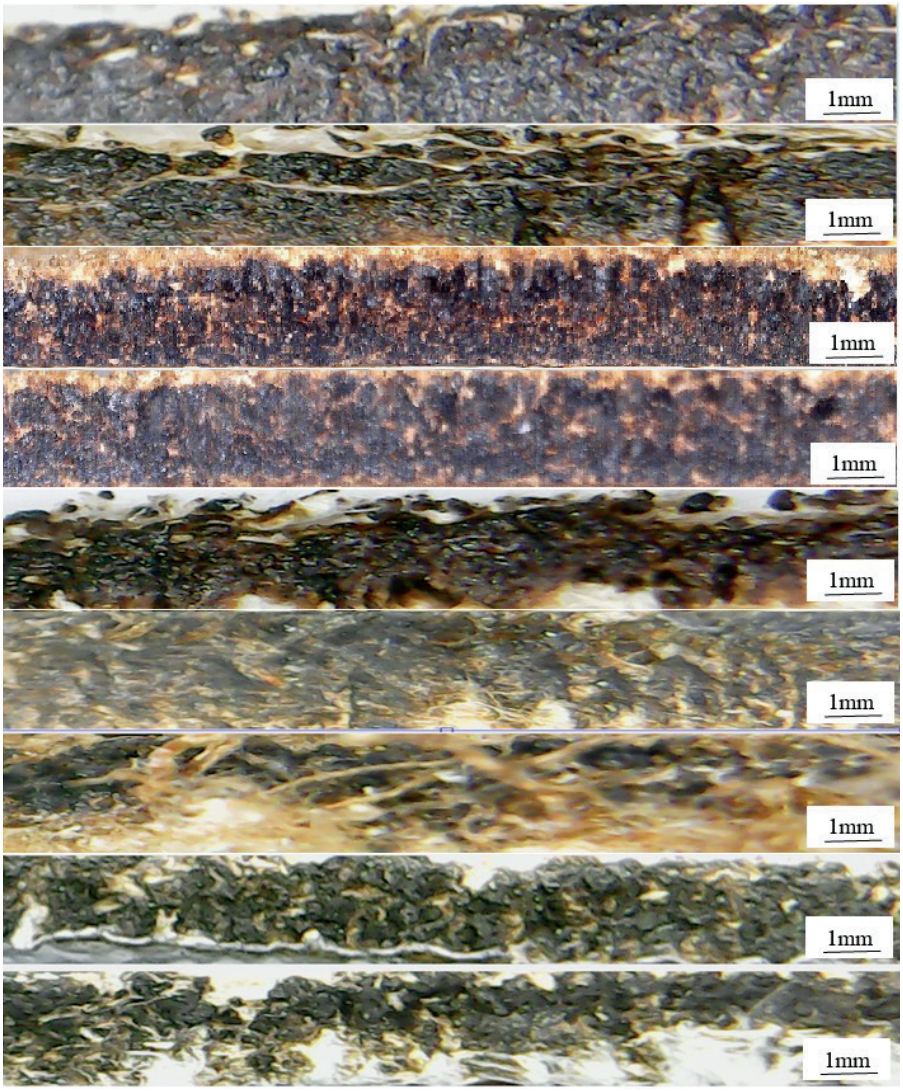

Figure 3. Examples of enhanced image of leather cross section

Enhancement of acquired images

The image enhancement is the next step after image acquisition. The acquired image is enhanced according to the requirements of the image processing software. This could assist in extracting maximum information from the captured image. Figure 3 shows the enhanced images with trimming using USB digital microscope. It is the process of enhancing the quality and information content of original data.The unwanted part in the image is taken off and only the area of interests are retained.

Conversion of color image to binary image

In the present study, MATLAB software package was used for image processing. It is a method of extracting particular characters or a number of specific details obtained from the acquired image. Figure 4 shows conversion methodology of captured image to binary image. The image processing begins with the conversion of an RGB image to a gray scale image, which is then transformed to a binary image. The image was captured in real time using a digital microscope. Every image was captured in RGB. The conversion of RGB scale to a binary scale with a set threshold over trial and error method was implemented. Every leather sample of varying color has a different threshold. Based on this threshold the image is converted into the binary scale (i.e. 0 and 1) where 0 corresponds to the dark region and 1 corresponds to the light region.

Design layout in diode based LBM

The goat leather of 1mm thickness was used in this present study owing to its significance in the industrial production system. The input and output process parameters can influence the productivity measurement. Power (P), Frequency (F), Amplitude (A), Duty Factor (D), Cutting Speed (C) have been chosen as the input process parameters for the present investigation due to their importance in the LBM process.

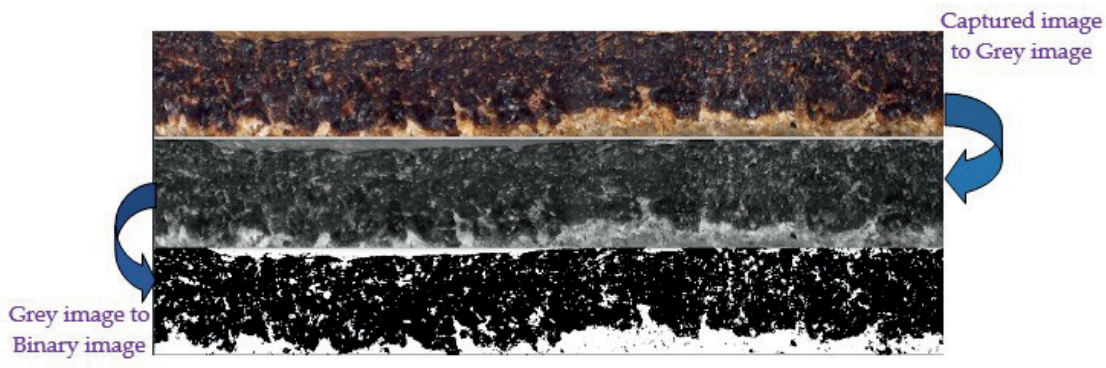

Figure 4. Conversion methodology of captured image to binary image

Table I

Input Process Variables

Process Parameter	Symbol	Unit	Values
Power	P	Watt	20
Frequency	F	Hertz	3000,6000,9000,12000,15000
Duty Factor	D	%	17,34,51,68,85
Amplitude	A	Voltage	3,3.5,4,4.5,5
Cutting Speed	C	mm/s	200,210,220,230,240

Table II

Design layout in Power diode based LBM

Trial no	Power (W)	Frequency (Hz)	Duty cycle (%)	Amplitude (V)	Cutting speed (mm/min)
1	20	3000	17	3	200
2	20	3000	34	3.5	210
3	20	3000	51	4	220
4	20	3000	68	4.5	230
5	20	3000	85	5	240
6	20	6000	17	3	200
7	20	6000	34	3.5	210
8	20	6000	51	4	220
9	20	6000	68	4.5	230
10	20	6000	85	5	240
11	20	9000	17	3	200
12	20	9000	34	3.5	210
13	20	9000	51	4	220
14	20	9000	68	4.5	230
15	20	9000	85	5	240
16	20	12000	17	3	200
17	20	12000	34	3.5	210
18	20	12000	51	4	220
19	20	12000	68	4.5	230
20	20	12000	85	5	240
21	20	15000	17	3	200
22	20	15000	34	3.5	210
23	20	15000	51	4	220
24	20	15000	68	4.5	230
25	20	15000	85	5	240

Diode based LBM method has been used to cut the leather material. The 20 Watt diode laser emits a beam of wavelength 450nm. The laser diode has the optical power of 5.5W and LD+C-lens light source. The laser diode can be triggered using pulse width modulation (PWM) approach. The power was maintained constant at 20W for all the trials. Table I shows a list of the input process parameters and their corresponding ranges. As shown in Table II, the cutting experiments were conducted using power diode based LBM. The controlling parameters are used to correct errors in the system and to provide the best possible outcomes by changing each parameter individually. The electrical parameters are power, frequency, duty factor and amplitude and the cutting speed belongs to the mechanical parameter. The duty cycle determines the pulse width of the signal. The duty cycle is usually stated in percentage terms. Since duty cycle is a critical control parameter that determines the quality and length of the cut, it is essential to accurately generate the necessary duty cycle in percentage. The frequency determines how often the signal is repeated over time. It is related to repetition of the signal. Amplitude is a power modulator measured in terms of peak to peak voltage. The cutting speed refers to the laser module movement in the appropriate direction to cut the leather. It is measured in mm/min.

Results and Discussion

The goat leather was machined into rectangular specimens using 20W power diode based Laser Beam Machining with the optical power of 5.5W and LD+C-lens light source as illustrated in Figure 5. The laser diode can be triggered using pulse width modulation (PWM) approach. The photo diode laser based LBM process has

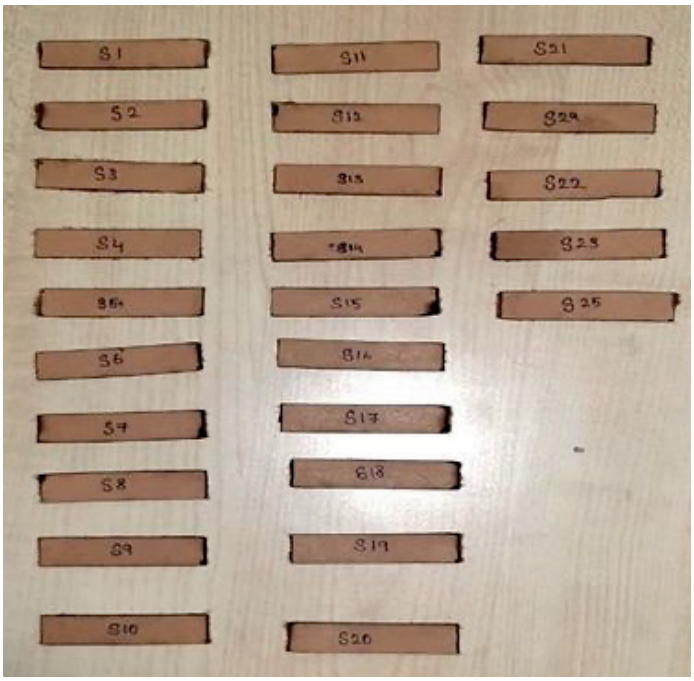

Figure 5. Machined goat leather using power diode based LBM

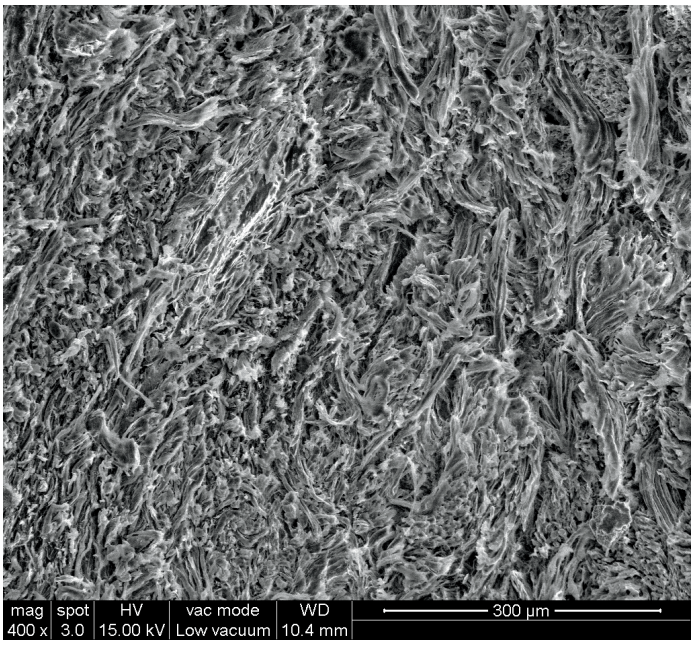

Figure 6. Machined leather surface using scanning electron microscope

created lower region of heat affected zone as shown in the scanning electron microscope image in Figure 6. The surface morphology of machined leather was observed with dross and striations of natural skin layer. The working of the laser machining begins with the software which controls the X and Y axis movement of the laser head. The required geometry of the cut was fed into the software as an image or G-codes. The laser was mounted on the movable mount in the CNC. The power of the laser can be controlled with the help of the software whereas the other input parameters of the laser such as frequency, amplitude, duty factor and cutting speed are given with the help of the waveform generator. The waveform generator is used to give preset precise input to test the laser in different working conditions. The CNC setup can be fully operated and controlled using the software. The stepper motors move accordingly such that the laser head moves in a coordinated motion along X and Y direction.

Calibration of USB digital microscope

The USB-microscopic camera was primarily calibrated and fixed to the base for maintaining a stable position. This was suitable for capturing the image of laser cut leather edges. The digital camera acquired many images with internal software. This algorithm automatically adjusts the focal length and focal measures based on the optimal focus measures. Hence the acquired images were not in identical focus owing the external constraints with the same light source. The intensity was varied due to the different carbonization made by the process factors. Once the image acquisition was done by the camera, the acquired images were transferred to a computer using software called Celestron micro-capture pro. Then the images were uploaded into the MATLAB programming language

for the image processing. The acquired image was converted into a binary image to remove the RGB information in the image, since it is unnecessary with higher processing time. While converting to a binary image, the background of the image was also removed as it makes it difficult on determining the Heat Affected zone. The camera was calibrated to desirable level while capturing the image for attaining the maximum details via image, lighting, focus and height from the object. These are the parameters that can be varied in microscope camera to get the desired image. As lighting is one of the main aspects of image acquisition, it is very important to capture the image with adequate lighting for image processing. The lens was surrounded by an array of LEDs. These LED are adjustable which helps in varying the lighting intensity according to the needs. Focusing the camera is also important because it helps in attaining a clear image. The microscope camera is provided with a provision to adjust the focus to the desired level. As the camera is held in a stand, it allows the user to adjust the height from the material. There is a two way adjustable height which helps in maximum flexibility during image acquisition.

Image Processing of the specimens

The image of laser cut edge was taken for further processing. This was achieved with the help of the microscopic camera. The leather was placed in such a way that the camera captured the cross section portion cut edge of the leather. This was done with the help of clamps which were provided with the microscopic camera. The acquired image was trimmed such that the unwanted portions were cropped to do further processing. Once the image was inside the MATLAB program, the algorithm checks the grey scale value of each pixel. Then it was compared to the threshold value that had been set. If the value of a pixel fell below the set threshold value, then that pixel can be converted into white.

Table III

Measurement of carbonization percentage

Trial No	Captured Image to binary image conversion	Carbonization (%)	Unaffected Zone (%)
1		74.401030	25.598970
2	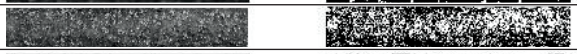	73.636899	26.363101
3	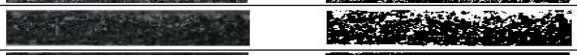	72.850000	27.150000
4		80.973508	19.026492
5	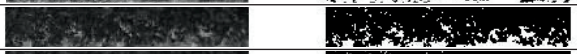	72.969429	27.030571
6	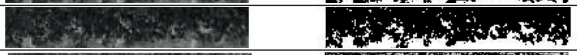	80.351171	19.648829
7		79.097849	20.902151
8	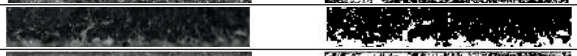	78.048891	21.951109
9		80.522229	19.411111
10		73.294004	26.705996
11		74.549662	25.450338
12	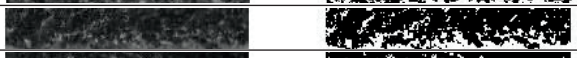	71.539992	28.460008
13		77.778884	22.221116
14		75.086345	24.913655
15		80.222117	19.777883
16		85.438596	14.561404
17	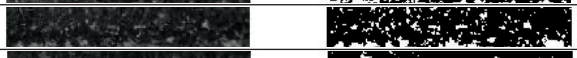	81.736767	18.263233
18	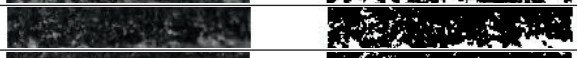	77.899338	22.100662
19		80.608952	19.391048
20		80.547561	19.452439
21	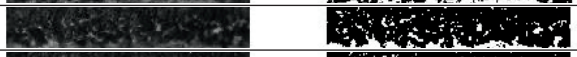	78.274000	21.726000
22		80.370000	19.630000
23	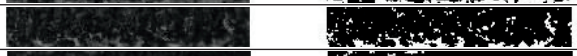	80.434783	19.565217
24	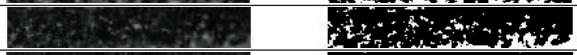	80.057062	19.942938
25		76.387928	23.612072

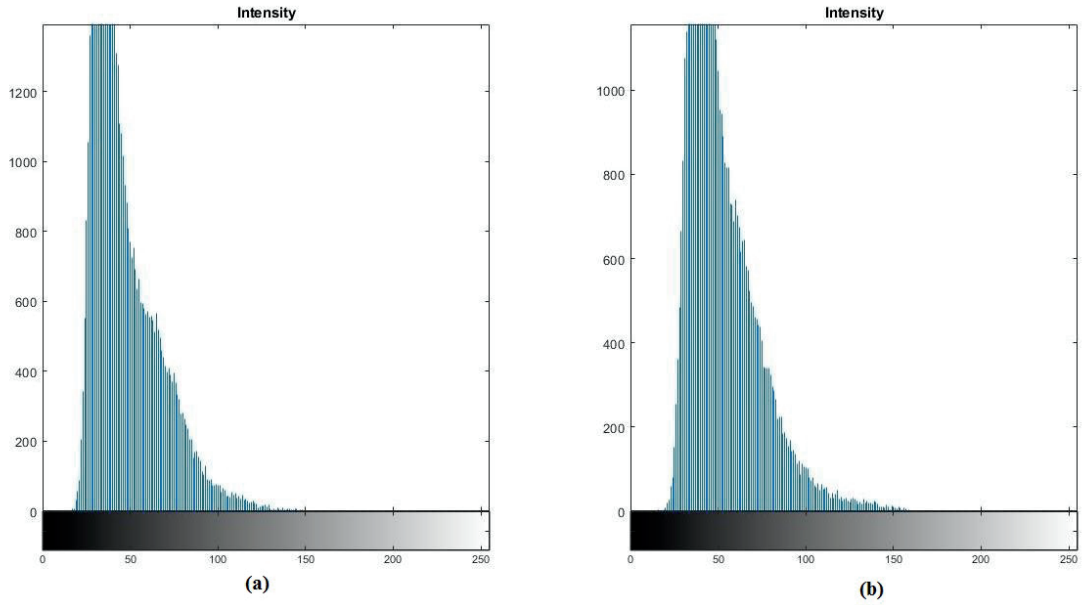

Figure 7. Histogram analysis for **(a)** Trial 1 **(b)** Trial 2

In the case of the value of a pixel being greater than the set threshold value, then that particular pixel was converted to black and accounts for the carbonization. The percentage of the carbonized and non-carbonized region was calculated by counting the number of white and black pixels and was displayed at the end of the algorithm.

Programming Techniques on the measurement

The leather samples were cut using a 20 W diode laser for the different input parameters. After the machining process, each and every sample's image was captured and processed to determine the percentage of carbonization. The images captured and processed for different samples are shown in Table III. In MATLAB, histograms are used to determine the range of gray level occurrences in a grayscale image as shown in Figure 7. It shows the distribution of pixels in the grayscale image, since each pixel value varies from 0 to 255. The value of 0 being the darkest and 255 being the lightest. The histogram was used to illustrate distribution with a range of 0 to 255 in the graphical format. Since the carbonization is not uniformly distributed throughout the leather after the machining process, a histogram is used to plot the distribution in a graphical form. It can be observed that the machined leather has grey scale values lying slightly towards the dark-side, this account for the carbonization effect that takes place during the laser machining process. The output parameters such as carbonization and non carbonized zone in terms of percentage were calculated.

Effects of process parameters on carbonization

The effects of process parameters on carbonization can be analyzed using main effects plot analysis. In the present study, the main

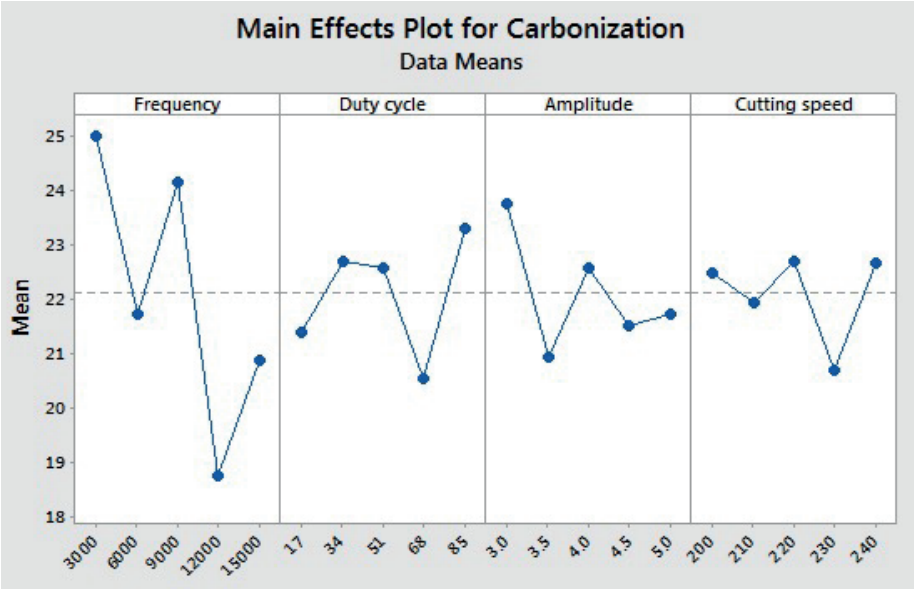

Figure 8. Main effects plot analysis on carbonization

effects plot analysis was performed with the help of Minitab 17 software package (State College, PA) as shown in Figure 8. The deviation of the mean response line with the horizontal line indicates the impact of the factors on the carbonization formed over the leather specimens. It was inferred that the PWM frequency has higher influential role on determining carbonization over the machined leather specimens. Since the PWM frequency determines the laser energy, it could determine the level of carbonization over the machined surface of leather specimens. Since the trial number 12 could produce lower carbonation region, it can be termed as optimal process factors combination. The lower duty cycle reduces the thermal energy. The lower duty cycle with moderate PWM and amplitude could produce lower carbonization layer. Hence trial 12 could produce better performance measures among the chosen process factors combination. The lower cutting speed and amplitude could produce higher carbonization owing to the higher thermal energy. Hence trial 16 could produce higher carbonization among the chosen process factors combination.

Conclusions

An experimental investigation was performed to analyze the effect of laser power diode on carbonization. From the experimental analysis, the conclusions made:

The technique of measuring carbonization can be used effectively in the leather industry for the accurate measurement of carbonization.

The lower duty cycle with moderate PWM and amplitude could produce lower carbonization layer. However, the lower cutting speed and amplitude could produce higher carbonization owing to the higher thermal energy.

PWM frequency has higher influential role on determining carbonization in leather cutting.

Acknowledgement

The authors would like to share their thanks and gratitude to M/s. Shafeeq Shameel & Co., Ambur, Tamilnadu, India for providing Vegetable tanned goat leather samples.

References

1. Stepanov, A., Manninen, M., Parnanen, I., Hirvimaki, M. and Salminen, A.; Laser cutting of leather: tool for industry or designers?. *Phys Procedia* 78, 157-162, 2015.
2. Nasim, H. and Jamil, Y.; Diode lasers: From laboratory to industry. *Opt Laser Technol* 56, 211-222, 2014.
3. Rodrigues,G.C. and Duflou,J.R.; Opportunities in laser cutting with direct diode laser configurations. *CIRP Ann Manuf Technol* 66, 245-248, 2017.
4. Vasanth, S. and Muthuramalingam, T.; Application of laser power diode on leather cutting and optimization for better environment quality measures. *Arch Civ Mech Eng* 21, 54, 2021.
5. Vasanth, S. and Muthuramalingam, T.; A study on machinability of leather using CO_2-based laser beam machining process. In: Advances in manufacturing processes lecture notes in mechanical engineering. Singapore: Springer; 239–44, 2019.
6. Malhotra, A., Gupta, S., Vasanth, S. and Muthuramalingam, T.; Adaptive Focal Length Laser Tuning Method for High Precision Cutting," *2020 IEEE 7th Uttar Pradesh Section International Conference on Electrical, Electronics and Computer Engineering (UPCON),* 2020, pp. 1-4, doi: 10.1109/UPCON50219.2020.9376428.
7. Muthuramalingam, T., Vasanth, S., Gupta, S. and Pi, V.N.; Genetic algorithm based optimization of cutting parameters in CO_2 laser beam cutting of cow leather. In: Advances in engineering and application lecture notes in networks and systems.Springer, Cham; pp. 485-490, 2021.
8. Varghese, A., Jain, S., Amalin Prince, A. and Jawahar, M.; Digital microscope image sensing and processing for leather species identification, *IEEE Sens* 20, 10045-10056, 2020.
9. Sakaev, I. and Ishaaya, A.A.; Diode laser assisted oxygen cutting of thick mild steel with off-axis beam delivery, *Opt Laser Technol* 138, pp.106876, 2021.
10. Tatzel, L., Tamimi, O.A., Haueise, T. and Leon, F.P.; Image-based modelling and visualization of the relationship between laser-cut edge and process parameters, *Opt Laser Technol* 141, 107028, 2021.

H.E.A.T.
A New Sustainable Green Solution for Treating and Evaporating Hide Brine Wastewater

by
Russell Vreeland* and John Long
Eastern Shore Microbes, Belle Haven, VA, USA

Abstract

Salt curing of hides releases a significant amount of excess water that must be disposed. In larger abattoirs this can result in production of tens of thousands of gallons of saturated salt brine that is also contaminated with biological material from the hides. These brines are often stored in enclosed impoundments that ultimately fill and need replacement, or the facility must build multiple impoundments. The proprietary, biologically based, sustainable *Halophilic Evaporative Applications Technology (H.E.A.T.)* process has been developed as a method to accelerate the evaporation of salt saturated brines. The process has been tested for 18 months in a full-scale lagoon located at an operating American beef plant. The process successfully evaporated an additional 31.99 inches of brine (866,900 gal) acre^{-1} of concentrated hide brine in one year, nearly drying out the South lagoon. Ambient evaporation of the same brine in an identical control lagoon at the site was only 19.19 inches (520,000 gallons) acre^{-1} representing a 1.66× increase in brine evaporation from the *H.E.A.T.* microbes. During 2020, the plant produced 3,376,000 gallons of brine, meaning *H.E.A.T.* evaporated 100.4 % of plant production in one lagoon in its first year. This was accomplished without additional infrastructure, equipment, or external heating. During this test, Biochemical Oxygen Demand in the lagoons decreased over 98% with concomitant odor reduction. Beginning in October 2020, the lagoon began receiving all brine produced daily by the plant. This continued over the winter period, during which time the process evaporated over 34% of the inflow. Continued fertilization and microbial augmentation are essential for the continued healthy development of the system. Overall, the process and its essential microbial populations were stimulated by continuing inflow of fresh hide brines. The microbial process increases brine evaporation of concentrated salt brines, reduces odors and represents a new environmentally friendly mechanism for solving an industrial problem that has long plagued hide producers.

Introduction

The first description of a biological impact on evaporation rates actually occurred in 2500 BCE in China, where salt makers recognized that having their small pans turn red meant they would be able to harvest their salt within days rather than months.[1] This reddening is often seen in salt production situations[2] but its impact on the actual evaporation rate has been ignored prior to the Eastern Shore Microbes (ESM) developments described here. The H.E.A.T. process is based on developing custom culture and nutrient mixes for each class of brine to be treated or evaporated. The fertilizers and cultures are added to the lagoon to stimulate development of a huge population of microbes which can reach over 1 billion live cells in every milliliter (cc) regardless of the size of the lagoon. One likely mechanism for the process is that the actively metabolizing microbes give off excess metabolic energy as heat and increase the temperature of the brine much like typical compost piles. Alternatively, or even concomitantly, the dense biomass makes the lagoon red. This biomass reflects the hottest wavelengths of sunlight into the water increasing the brine temperatures even more. Neither of these mechanisms have been proven at this time but both are likely mechanisms for the process. There are additional possibilities ranging from the microbial movement causing microscopic disruption of the brine surfaces and/or microbial by-products that lower the surface tension resulting in more rapid evaporation or possibly the microbes themselves acting as foci for crystal formation causing the salt to precipitate more quickly than an uninoculated lagoon. Now that this acceleration has been documented these various mechanisms can be investigated.

Salt curing of hides prior to tanning has been used by the industry for many years. During this curing process, hides will release a significant amount of water into the raceways. While hide production was carried out in small operations, this excess brine was also a relatively small problem. As processing plants increased to ever greater head kill, the problem became more acute. Especially since the evaporation rate of water decreases as the concentration of salt increases evaporation may be retarded, as much as 0.71 for NaCl.[3] Due to multiple moving and opposing solid, liquid gas interfaces estimating evaporation in large open lagoon areas is difficult. As evaporation reduces the overall brine volume in a lagoon, it tends to force the brine surface lower in the lagoon. However, in saturated hide brines, evaporation causes salt precipitation, so that large scale salt deposition displaces the brine surface, pushing the air brine interface back upward. At the same time, large lagoons must be designed with sloping sides of different ratios depending upon

*Corresponding author email: rvreeland@esmicrobes.com
Manuscript received August 3, 2021, accepted for publication September 21, 2021.

the soil type surrounding the lagoon. This slope means that as the brine surface falls, there is a smaller overall evaporative surface and every cm (or inch) of drop represents a lower volume than the preceding cm (or inch). But since the salt layer is moving opposite to the surface, every cm (or in) of gain actually represents more volume displacement than the unit below. Finally, random but certain rainfall raises the water level, and may dissolve the underlying salt or it may actually form a low-density layer at the top of the brine. Once again, measuring this volume is not straightforward as lagoon liners are stretched above the lagoon berm directing rainfall into the lagoon from a surface area that may be significantly larger than the brine surface itself.

Consequently, following evaporation (and enhancement) requires monitoring all of these systems over time and with consistent measuring activities. This manuscript describes a study conducted on two large lagoons, filled with hide brines, during which these various parameters were followed over time. The data demonstrate that the proper microbial population does indeed significantly increase evaporation while simultaneously biodegrading the organic contaminants in the hide brine.

Goals of Hide Brine Treatment: In order for any treatment to be effective as a solution to problems of brine disposal, the process must achieve certain specific goals. These include: enhanced evaporation; allowing smaller (or fewer) lagoons; reduction of Biochemical Oxygen Demand (BOD) with concomitant odor reduction; and finally, creating an evaporative environment that can keep up with plant production.

Materials and Methods

Purpose of the Project

This project was originally designed as a full 1 year to 18-month demonstration study. However, after being started the project was interrupted for several months by the Covid-19 pandemic and by plant closures during that time. One of the primary goals of the project was to determine if the H.E.A.T. process evaporated brine during the colder months of the year. The test site was at an active hide production facility in Northeastern Colorado.

Hide Lagoons

The hide lagoons used were each 4.8 acres in surface area and designed to hold up to 15,000,000 million gallons of brine. At the time of this project, each lagoon had been in use for nearly 30 years and each had built up thick layers of salt. These lagoons were chosen because each was being prepared for repair or decommissioning.

One lagoon (designated South) was chosen as the test site and its companion (designated North) was chosen as the control. The H.E.A.T. process was initiated in the South lagoon using proprietary custom designed mixes of culture and matching nutrients in August 2019. North Lagoon received no microbial or nutrient treatments. North Lagoon therefore, provided a measure of the ambient evaporation rate of untreated hide brines. Following this first inoculation, both the North and South lagoons were taken out of service to allow all parties to evaluate the events and document the changes that the H.E.A.T. system would foster. Due to the need to build the proper biomass and fertilization conditions, no measurements were taken until the system was ready. Originally, due to having a volume of nearly 2 million gallons in the test lagoon and beginning the biological process so late in the year this was planned to require up to five months. However, following a second inoculation and fertilization of the South Lagoon in October 2019 the biomass development occurred sooner than expected so the measurements began in November 2019. To begin the formal test both lagoons received additional brine from another hide lagoon. This decision was made due to the fact that the South lagoon was already drying and all personnel involved wanted to collect more data. Each lagoon was filled with several days' pumping. The plant utilized the same pump/hose system and pumped for the same lengths of time which was done to provide each lagoon with an equal amount of fresh brine. Standardized sampling points were then established in each lagoon, using three PVC pipes driven into the underlying salt pack to provide those sampling points. The PVC pipes were placed roughly in a line running along a north to south transect of each lagoon. From that point on, all measurements were taken by boat next to those pipes. Depth measurements were taken using a weighted 8-inch Secchi disk to provide a flat measurement that was less impacted by the rough bottom of the lagoon. Brine samples were sent to the ESM home laboratory for analyses on a monthly basis. Field measurements were obtained from the boat and all brine samples were obtained by an on-site water treatment operator.

A third and final inoculation and fertilization of the South lagoon occurred in the final week of May 2020 in order to prepare the system for the coming summer. No additional fertilizations, inoculations, or brine additions occurred between this May date and September 2020. Pond volumes were still monitored during this period although once again the frequency was impacted by Covid-19 outbreaks.

A second short term extension of the demonstration was initiated for the period of October 2020 to March 2021. This portion of the demonstration focused on the potential of the lagoon to begin receiving all of the excess hide brine coming from the plant.

Evaporation Measurement

To facilitate these measurements, a Computer Aided Design (CAD) table was generated using lagoon blueprints. The table was accurate to 0.01-inch levels in the ponds. The brine surface position for each measurement date was obtained using daily staff gauge measurements in each lagoon. The position of the salt pack was determined from

the depth measurements using the weighted Secchi Disk at the three locations within each lagoon. Since the salt pack proved to be dish shaped with a deeper center in each lagoon, these measurements were averaged for each data point. Precipitation measurements were taken from the daily staff gauge reports provided.

These various numbers were treated as follows: each daily staff gauge measurement was converted into a measure of decimal feet and the total pond volume for that point was obtained using the CAD table. Once the average brine depth was obtained from the Secchi readings, the position of the salt pack was determined by subtracting the average depth from the overall brine surface position. The displacement volume of the salt pack was then obtained using the CAD table. The overall volume of brine remaining in the lagoons was then determined by subtracting the salt displacement volume from the total predicted volume given by the staff gauge reading.

During the project an additional factor in estimating evaporation in the South lagoon arose as the accelerated rates in the lagoon caused the salt pack to be exposed in an ever larger "beach." This was noted in March of 2020 and was only occurring in the test lagoon, not the control. Therefore, the best approach was not to add additional brine to the lagoons (since the control lagoon did not have a beach) and attempt at times to measure the extent of this beach. This proved to be extremely difficult to accomplish on a consistent basis but some estimates were obtained. In March of 2020 the beach was found to be 12 feet wide. The beach grew to be (50 ft) on a side by July 2020 and 75 ft by September 2020. An estimate of the evaporative surface of the South Lagoon was performed using equation 1.

(1) $Surface\ area\ of\ Brine = (459 - 0.95(D+L))^2$ where
D = estimated width of salt exposure
L = Exposed area of liner (calculated by subtracting staff gauge measures from design lagoon depth (12 ft).
459 = total length of the sides of the lagoon at the 12 ft interval.

Once again, this problem was not faced in the control North lagoon as the brine continued to remain in contact with the pond liners throughout the test period.

Bacterial Populations

Bacterial biomass was followed using standard surface spreads on CAS agar[4] supplemented with 20% (w/v) NaCl. All samples were decimal dilutions, with 0.1 ml of each dilution surface plated onto the CAS medium. Plates were incubated inside plastic bags (to increase humidity) at 35°C for at least two weeks to allow for the slower growth of cultures.

Biochemical Oxygen Demand (BOD)

BOD analyses were based on procedures described in USGS TWRI Book 9 Chapter A7[5] and Standard Methods for Water and Waste Water analysis 5210[6] with the following modifications to account for the high salinity of the brine. Diluent was prepared with 20% NaCl and sterilized. Dissolved Oxygen was measured using an RDO probe system, corrected for salinity and calibrated after each dilution and sample. Proprietary culture mix HS 001 was used as a seed culture. While BOD is an important measure of waste water treatments, this has proven to be one of the most difficult assays in these brines. This appears to be largely due to the heterogeneity of the materials. The brines contain significant amounts of dirt, blood and other coagulated materials that contribute to the overall BOD and do not evenly distribute in the BOD diluent. Therefore, one bottle of a replicate may show measurable BOD while a second bottle with the same sample volume may, following incubation, have no oxygen remaining. In order to provide some measure of stability for this assay we adhered strictly to the normal analytical criteria. After 5 days of incubation at 20°C, data is acceptable if all of the following criteria are met: 1) bottles must have at least 1.0 mg/L Oxygen remaining; 2) the second reading of dissolved Oxygen must be at least 2.0 mg/L below the first reading [i.e. a loss of at least 2.0 mg O_2/L]; 3) No apparent toxicity in more concentrated samples; 4) no data anomalies in a set of replicates [i.e. one bottle with no Oxygen loss and one with total oxygen loss]. Throughout the study, and given the high organic levels in the brine Rules 1 & 2 proved the most difficult to meet consistently.

Loss on Ignition

Loss on Ignition (LOI) is a bulk measure of the organic fraction of a sample after it has been dried at 120°C then incinerated at over 600°C to convert all carbon- containing materials to CO_2 and H_2O or other gasses. Measurement of this parameter did not begin until May 2020 so there is somewhat limited information. Loss on ignition studies were conducted using the procedure described by Heiri et. al[7] using only 6 crucibles. No attempt was made to determine carbonate content in these brines.

Results

Evaporation

Photographic examination of the South Lagoon demonstrated significant evaporation in 9 months (Figure 1). Evaporation in the South lagoon exceeded that in the North by a considerable amount. As shown in Figure 1, at the start of the case study, brine in the South lagoon was in contact with the lagoon liner. A similar situation was seen in the North Lagoon. By March 2020, the South Lagoon brine had receded from the liner and a "salt beach" several yards wide had appeared around the lagoon. Brine in the North lagoon was still in contact with the liner (image not shown). By the end of this first trial the South Lagoon showed a beach nearly 75 ft wide. The North Lagoon did not have a visible beach.

This result led to a decision to conduct a short follow-on study, using the drying South lagoon for active brine disposal. The goal of this portion of the testing being to determine if the single South Lagoon could evaporate fast enough to keep up with plant hide brine

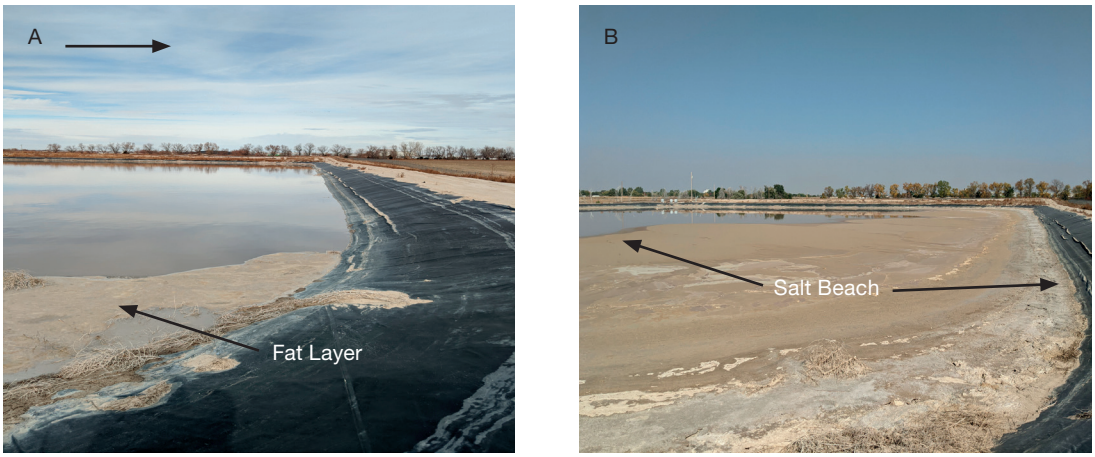

Figure 1. Evaporation development in South Lagoon over the initial 11-month study. **(A)** Left image November 2019; **(B)** right image September 2020. Black arrow in left figure shows North for both images

production. Unfortunately, due to the Covid-19 pandemic, this testing could not begin until October 2020 and was supported through March 2021 when funding terminated. At the point of termination, the brine depth of the South Lagoon was 9.83 ft on the installed staff gauge. This level, was identical to the brine readings for South Lagoon on 9 December 2019. At this level, the South lagoon contained 3,653,070 gallons of liquid. In March 2021 this level was reached with only 2,074,019 gallons (Table I). The difference in these volumes was caused by salt accumulation from evaporation in the 2019/2020 test.

Images of the progression of evaporation in the South lagoon showed a striking development of a salt "beach" that began to develop within 3 months of inoculation of the lagoon. Figure 1A shows the condition of the lagoon at the beginning of the demonstration project. Brine was touching the pond liner at all points, interrupted only by layers of accumulated fat (lower left in 1A). Within two months of inoculation, this fat layer was degraded and odors emanating from the brine were noticeably reduced. By March of 2020, a 12 ft wide salt "beach" that extended around the entire lagoon had developed. By September of 2020, this "beach" area extended out nearly 75 ft around the lagoon (Figure 1B).

Calculations based on brine depths indicated that the South Lagoon had evaporated 31.99 inches of brine from November 2019 – October 2020. Much of this evaporation occurred after the growing salt beach began to reduce the evaporative surface of the South Lagoon. During this project, the surface area of the South Lagoon decreased from the initial 4.8 acres to 3.4 acres (average 3.84 acres). More importantly the evaporation rate per acre actually increased even with the smaller surface area (Table I). By contrast, the North lagoon evaporated only 19.19 inches of brine in a larger and constant surface area over the same time period (Table II).

By September 2020, the South Lagoon reached an evaporation rate of over 6,000 gallons of brine ($acre^{-1}$ day^{-1}). Comparison of this level with the 105 - year average fresh water evaporation for this area

Table I

Evaporation in treated South lagoon over first 9 months of 2020.

Date	Surface area of brine (acres)	Evaporation (gal/acre)	Acre inches evaporated	Sampling interval (days)	Evaporation (gal/acre/day)	FW evaporation (Month[1])
12/9/19	4.8					
1/13/20	4.8	64,583	2.38	36	1794	0.00
2/14/20[2]	4.8					0.00
3/4/20	4.6	93,478	3.45	20	4674	1.75
5/21/20	4.3	83,721	3.09	98	854	6.96[(3)]
6/16/20	4.2	119,048	4.40	27	4409	4.42[(3)]
7/10/20	4	82,500	3.04	25	3300	4.84
9/17/20	3.4	423,529	15.63	70	6050	7.57[(4)]
Final total		866,859	31.99		3,514 (Avg)	28.73

1: Monthly Fresh Water (FW) evaporation in the local area over 105 years. These values have been corrected from Class A Evaporation pan readings by multiplying pan readings by 0.7 as described (8); 2: Depth measurements indicated a gain of brine in this lagoon for this date but no corresponding gain was detected in the adjoining lagoon. Therefore, these lines have been omitted; 3: Values for any month with two sampling dates have been combined; 4: Evaporation for multiple months have been added for these samples.

Table II

Evaporation in untreated North lagoon over first 9 months of 2020

Date	Surface area of brine (acres)	Evaporation (gal/acre)	Acre inches evaporated[1]	Sampling interval (days)	Evaporation (gal/acre/day)	FW evaporation (Month[1])
12/9/19	4.8					
1/13/20	4.8	0	0	36	0	0.00
2/14/20	4.8	18,750	0.69	32	586	0.00
3/4/20[2]	4.8					1.75
5/21/20	4.8	77,083	2.85	98	787	6.96[3]
6/16/20	4.8	107,708	4.38	27	3989	4.42
7/10/20	4.8	60,416	2.23	25	2417	4.84
9/17/20	4.8	256,250	9.45	70	3661	7.57[4]
Final total		520,270	19.19		1,907 (avg)	28.3

1: Monthly Fresh Water (FW) evaporation in the local area over 105 years. These values have been corrected from Class A Evaporation pan readings by multiplying pan readings by 0.7 as described (8); 2: Depth measurements indicated a gain of brine in this lagoon for this date but no corresponding gain was detected in the adjoining lagoon. Therefore, these lines have been omitted; 3: Values for any month with two sampling dates have been combined; 4: Evaporation for multiple months have been added for these samples.

showed that the H.E.A.T. treated lagoon consistently exceeded fresh water evaporation for most of the measured months (Table I) once the measured pan rates were converted (0.7× pan measurements) to account for the larger lagoon size. The data also indicated that the microbially treated lagoon evaporated brine through December and January when fresh water evaporation is nil. During this period both lagoons received 131,500 gallons of precipitation per acre. This volume was not added to these calculations simply because both lagoons would have received the same amounts. Precipitation was added to the calculations for the second part of this case study because it focused only on the South Lagoon.

Table II reflects the same data points for the control North Lagoon. These data illustrate the expected effects of increasing salt concentrations in decreasing brine evaporation which is the main problem the H.E.A.T. process is designed to solve. Over the same time period, this identical lagoon evaporated only 19.19 inches of brine. Some surface area decrease did occur due to the wall and liner slope however conversion of the calculated square feet (using equation 1) to acres did not fall below the 4.8-acre value. More importantly, evaporation from the North Lagoon only exceeded a corrected fresh water rate on a single occasion, during summer 2020. But, as with Table I, this occurred during one of the two longest sampling intervals. This makes it difficult to determine if the measurements might have been caused by movement of the sampling boat, or measurement in a depression in the bottom. Overall however, evaporation in this lagoon never exceeded that of the South Lagoon, for any sampling point or any of the data calculations. Compared to fresh water the decrease in evaporation rate due to the concentrated salt was nearly 30%. Unlike South Lagoon; the North lagoon did not evaporate any brine during the winter period.

Given the data from the earliest part of the trial (Table I), indicating that the H.E.A.T. treatment did evaporate brine during the winter period, the test was extended to determine if this evaporation would continue with brine waste addition and to measure the extent of winter evaporation. At this time a drone with photographic capacity became available. Drone flights provided an overview of both lagoons. Waste brine was added only to the South Lagoon, so all measurement of North was stopped. The results of this demonstration and the responses of the H.E.A.T. cultures are shown in Figures 2 & 3 and in Table III. Daily brine addition began on 20 September 2020 and continued to the end of March 2021 when the demonstration ended.

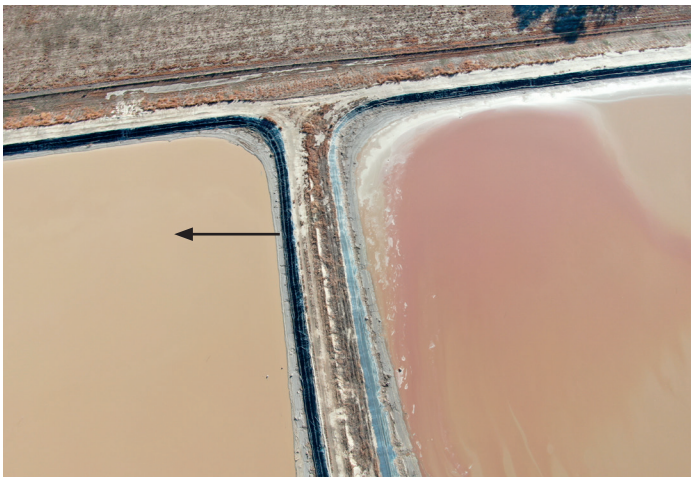

Figure 2. Aerial view showing both control and the test lagoon (North left; South right) on 29 October, 2020. The red plume in the right-hand image shows the bacterial bloom occurring as the microbes began to attack the inflowing brines one month after fertilization and addition of H.E.A.T. cultures. The white area along the top of the South lagoon is the remains of the beach as new brine fills the lagoon. Arrow indicates North.

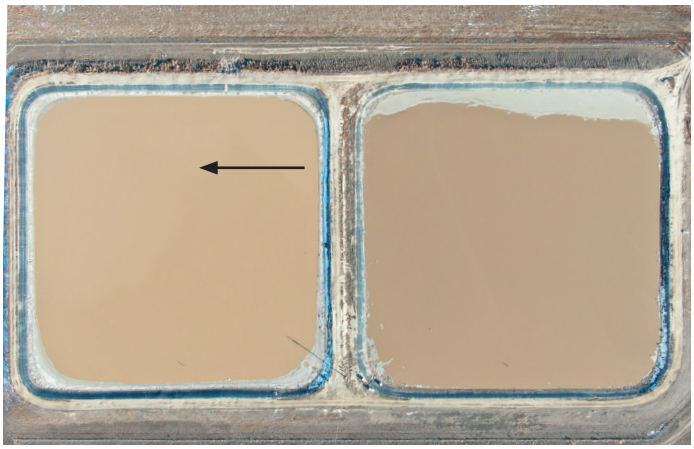

Figure 3. Aerial view (4 December 2020) of North (left) and South (right) lagoons. The red microbial plume seen in Figure 2 has now spread throughout the South Lagoon (hence the darker color of the brine). The white material at the Eastern edge of the South lagoon is the remains of the salt beach on that edge since brine enters the lagoon from the lower left corner of South Lagoon. Arrow indicates North.

During this brine addition phase, the plant released all of its daily waste brine (avg 20,000 gal day^{-1}) into the South Lagoon. Within the first month of additions, the microbial population responded in a dramatic manner as is shown in Figure 2. The ESM red cultures bloomed to a point where the population was most visible in the Eastern portion of the lagoon and could be seen mixing with the inflow plume (Figure 2).

As the additions continued the population became more diffused through the South Lagoon causing the brine to darken as is evident in Figure 3 (righthand lagoon).

During the 6-month long trial, the South Lagoon received 2.21 million gallons of hide brine waste, and over 970,000 gallons of rainwater (based on a 5-acre runoff area). This continuous addition made measuring the evaporation rate even more difficult than the previous part of the demonstration. Considering that the South Lagoon is a terminal pond and since no leaks were detected in monitoring wells it was possible to assume that all losses of brine occurred via evaporation. Therefore, by calculating the total inflow, then comparing it to the measured gain it was possible to obtain at least a base estimate of brine losses through evaporation. These data are shown in Table III. These data show that at the beginning of the trial the South Lagoon biomass did evaporate over 57% of added brine. However, as the rainfall increased (Jan. – Mar. Table III) and brine volumes began to build, this evaporation effect appears to have tapered to only 6 % in March 2020. The data did reveal that during brine addition and the winter period, fertilization was an important component of this process. Table III shows the sampling points that roughly correspond to fertilization events. However, the fertilizations all occurred prior to the sampling dates. The project began with the addition of 550 gallons of fertilizer on 22 October 2020, over a month before the first sampling. The fertilization corresponding to the 4 Jan 2021 sampling also included 550 gallons of nutrients added on 23 Dec 2020 (nearly 2 weeks before the sampling). The final fertilization incorporated only 275 gallons of material and occurred on 25 Jan 2021, 21 days prior to sampling. In all cases the detected evaporation appeared to accelerate but was followed by a significant decrease in the rate as more brine (and rainwater) flowed into the lagoon diluting the added nutrients. The evaporation data in Table III indicates that while the ratio of nutrient to inflowing brine was around 0.05 : 0.06% (fertilizer : inflow) (Jan – Feb Table III) significant evaporation occurred despite the winter season. When this level dropped to only 0.03% in February 2021 a good evaporation rate was still detected however, this appeared to drop quickly to only 6% in March when no additional fertilization was provided.

Bacterial Populations

At the beginning of these trials the bacterial population in the brine for both lagoons was very low at 3.6×10^3 ml^{-1} total colony forming units (TCFU) and only 5.0×10^2 red colony forming units (RCFU) ml^{-1}. Once the treatments began these numbers began to increase. By March of 2020 the population in the South lagoon had increased over 1,000-fold to over 3.8×10^6 TCFU ml^{-1}, a major part of this total 1.2×10^6 RCFU ml^{-1} being the red cultures needed to accelerate evaporation rates. Due to warmer weather and the fresh brine added in December (2019) bacterial populations in the North lagoon increased to 1.7×10^5 TCFU ml^{-1} and 4×10^4 RCFU ml^{-1}. The project was placed on hold due to budgetary issues so continued fertilization and care of the cultures ceased. A May 2020 sample showed that the biomass had dropped significantly in the South lagoon (2.23×10^4 TCFU ml^{-1}; 1.27×10^4 RCFU ml^{-1}). Since negotiations were underway to continue the trial an additional fertilization was provided. North lagoon population dropped to pre-trial levels (1.1×10^3 total colonies/ml^{-1} and 3.7×10^2 red colonies/ml).

Treatment of the South lagoon began again in October 2020 for an additional 6 months at the request of the facility and to complete an 18-month total measurement period. After the first supplementation the population rebounded to 7.3×10^4 TCFU ml^{-1} and 2.9×10^4 ESM microbes RCFU ml^{-1}. By the end of December 2020 with continued nutrient and culture additions, the populations in South Lagoon continued to increase reaching 5.1×10^6 TCFU ml^{-1} and 3.0×10^5 RCFU ml^{-1}. This population reached levels that became visible to the naked eye (Figures 2 and 3) and was maintained there through the end of the trial.

Biochemical Oxygen Demand (BOD)

All early samples from these ponds showed extremely high levels of BOD with both lagoons running above 170,000 mg O_2/L. By May 2020 both lagoons showed a decrease in BOD (note neither lagoon was receiving fresh waste at this time but both had active native (North) and enhanced (South) microbial populations. North lagoon BOD showed 24,800 mg BOD/L while South reached 8,900 mg

Table III

South lagoon responses with all produced hide waste brines being added daily to the single lagoon. Some columns may not add up due to rounding errors while converting to decimal equivalents to reduce the size of the table. The full numbers are shown in the supplementary data files.

Date	Interval (days)	Precip. (mil. gal.)	Hide Brine added (mil. gal.)	Total water added (mil. gal.)	Lagoon Brine Vol. (mil. gal.)	Change in volume Between samplings (mil. gal.)[3]	Difference (actual - Theoretical) (mil. gal.)	% Evaporated (total vol. change/total added) × 100	Theoretical Staff Gauge (based on volume)	Staff Gauge (daily measure)
9/17/2020					0.75					9.00
11/3/2020	48	0.02	0.55	0.57	0.996	0.25	0.32	57[1]	9.38	9.00
11/25/2020	12	0.04	0.37	0.41	1.26	0.26	0.14	34	9.35	9.08
1/4/2021	41	0.37	0.39	0.76	1.72	0.47	0.29	38[1]	10.00	9.50
1/21/2021	17	0.03	0.26	0.29	1.97	0.25	0.04	14	10.90	9.58
2/16/2021	27	0.22	0.30	0.52	2.07	0.10	0.43	82[1]	10.10	9.75
3/3/2021	16	0.03	0.18	0.21	2.45[2]	0.38[2]			9.97	9.83
3/18/2021	15	0.26	0.16	0.42	2.84	0.39	0.03	6	10.35	10.08
		0.97	2.211	3.18	2.09[4]			35 (of total added)		

1: fertilization events that occurred during the study; 550 gallons added prior to November and January sampling; 275 gallons added prior to Feb sampling. 2: measurement showing lagoon volume gain in excess of total added. 3: Calculated by subtracting each measured volume from the previous measurement and rounding to hundredths (i.e. 0.01); 4: this number reflects the total volume gained over the test. The original 0.75 million gallons was subtracted from the total 2.84 in the final cell. The total evaporation (35%) was calculated by dividing these two volumes.

BOD/L. While both are a significant reduction South lagoon clearly has much less BOD. In October 2020 South lagoon began receiving daily influx of brine from the Hide Plant yet the BOD continued to drop as the microbial population remained active. By December 2020, South BOD had dropped to only 3,000 mg/L while North (which still received no fresh waste) still registered 21,200 mg/L. BOD testing was halted in January due to the increasing ratios of fresh brine entering the lagoon. This brine would bring additional high BOD into the lagoon causing this parameter to rise.

Loss on Ignition

Initial LOI experiments showed 25.7 and 26.7% total dissolved and suspended solids in the South Lagoon and North Lagoon respectively. Of that fraction, 2.5% was organic (South) with 2.1% organic in the North. This difference was likely due to the ESM biomass in the South Lagoon. The LOI in the South Lagoon remained at 2.5% organic fraction, into December 2020.

Discussion

This case study demonstrated that the H.E.A.T. process does accelerate the evaporation rates of hide brines in large and working storage lagoons. The data show that the microbial population increases dramatically as long as supplemental nutrients and culture augmentations are being provided. This became more apparent as the population dropped dramatically from March 2020 to May 2020 when additions stopped for budgeting reasons and due to the coronavirus pandemic. The combination of additional nutrients in May and presumably, the warmer summer weather helped maintain the microbes until treatments resumed, but questions remain about how much more evaporation could have occurred with proper maintenance throughout the year. While the microbial population rebounded dramatically once regular maintenance was re-started, the overall condition of the test lagoons (old, nearly filled with salt and with deteriorating liners) precluded a longer-term effort in this case. It also indicates that the process may well be better in the long run if the treated lagoons are receiving fresh brines plus the proper culture and nutrient supplements to compensate for materials being diluted by the in-flowing fresh brines. This would occur because in a static lagoon the microbes attack the residual organic fractions, reducing it to gasses and some biomass. This was evident from the extensive BOD reduction (172,000 to 3,800 mg O_2 /L that occurred during the test period). BOD levels in the 3,000+ range are still extremely high for a normal waste stream discharge: but considering the starting level this represents a 98% reduction, and would include a corresponding reduction in odors. Since the North lagoon received no treatment but was allowed to remain fallow some degradation also occurred in the North Lagoon but the remaining BOD was still significantly higher (21,200 mg O_2/L) than that in the South Lagoon. Having a large biomass did not however negatively impact the crystals being produced in the lagoon, as it added only 0.4% to the total organic fraction of the precipitating crystals. This was evident from the LOI results showing that the lagoon being treated produced crystals with an organic fraction of 2.5% compared with 2.1% in the North Lagoon. While no attempt was made to further

characterize the respective organic fractions, it is likely that the material in the North Lagoon came mostly from the original hides (probably complex proteins and fats); while that in the South was more microbial biomass from the BOD breakdown.

Regardless of the scientific and analytical results obtained during this project, the key bottom line is the evaporation increase. As is clearly shown in Figure 1 (left to right in the images) and the volume data in Tables I and II, H.E.A.T. treatment accelerated the evaporation rates during the project. The data obtained, indicate that the process increased the evaporation rate of brine in the South Lagoon by over 66% per acre (866,859 vs 520,270 gallons) but more importantly the rate achieved in the South Lagoon exceeded the local evaporation rate of fresh water which is a key comparative in designing evaporation lagoons. During the same period, plant records show that the plant produced the equivalent of 703,000 gallons (25.95 inches) per acre of hide brine meaning that evaporation from the H.E.A.T. process exceeded plant production in the first year. Therefore, based on the first year a single lagoon of less than 4.8 acres in size could actually evaporate the entire production from the plant. This was the focus of the final portion of the test as shown in Table III. Choosing the slowest period of evaporation to run this particular test was an unfortunate choice but reasoned on the basis that this would be the time of year most needing acceleration. At the same time all parties recognized that the pond would likely gain volume over the winter season but felt that this gain would be offset by added loss such that the lagoon would gain on the plant during the summer period. As Table III and Figures 2 and 3 show, this did indeed happen in the early portions of the test with the lagoon evaporating 34 - 82 % of the inflow at various points in the trial. Additional nutrients were not added after February for budgetary reasons and as shown in Table III the plant received significant late winter precipitation. In fact, based on a 5-acre run-off zone (including liner that extended over the berm in two months this rainfall equaled or exceeded (Jan, Feb, March) brine coming from the plant. This created a double problem for the process. First, the organisms used are very adapted to the extremely high salts and are inhibited or killed by fresh water (indeed the population dropped by a full log (to 10^5 TCFU and RCFU) between Feb and March 2021 despite receiving additional nutrient. While the fresh water will ultimately become saltier as the salt pack dissolves this lower density water will tend to float on top of the high-density brine further inhibiting brine evaporation, which will continue until natural mixing (by wind and/or temperature) mixes the lagoon. Once again, this is evident from the sudden drop off in evaporation in March 2021 (to only 6%). Two additional bits of information however, also point to the effectiveness of this process in that as Table III shows if the amounts of brine being added were not evaporated the pond staff gauge should have increased much more than was measured by plant personnel. These differences ranged from the measured readings being anywhere from 0.5 to over 1.0 ft. However, the March recordings were closer at 0.27 ft (3 inches). Finally, a comparison of the volume of brine present in the lagoon showed that in December 2019 with a gauge reading of 9.83 ft, South Lagoon held over 3.65 million gallons of brine. By March 2021, the same Staff Gauge measurement (9.83 ft) occurred when the lagoon contained only 2.45 million gallons (see supplemental tables). This meant that the salt pack had increased in size and now occupied an additional 1.2 million gallons of the pond. Given the solubility of salt (32% w/v) this would require nearly 3.6 million gallons of evaporation which is in excellent agreement with the overall measured evaporation.

Based upon all of the available data, images and measurements, the following conclusions are warranted. The H.E.A.T. process works and accelerates brine evaporation in an economically significant manner even in the first year of treatment. Especially in the first year of establishment, the microbial population and the overall treatment are very sensitive to continued nutrient supplementation. The process may well slow or backtrack if this treatment is interrupted. In addition to accelerating evaporation, the process also provides significant (98%) reduction in lagoon BOD. While the process and microbial populations needed, appear to be stimulated by continuing inflow, the system does require maintenance with ESM's supplemental recipes. During winter, even a treated lagoon will gain volume, but based on the first year's results, this gain should be compensated by increased summer evaporation. Further testing and continued measurement have not yet covered a full summer period. One collateral bit of information that must be considered in all of these systems, is that accelerating brine evaporation will cause treated lagoons to gain a larger salt pack. This always needs to be considered as it will somewhat shorten the design life of a specific lagoon. At the same time, the increased evaporation allows for fewer or smaller Lagoons or allows users to clean and maintain these lagoons well before the design life of the liners is compromised. Furthermore, while the salt produced in a hide lagoon should probably not be used for further hide curing, the material produced does appear to be of sufficient quality for some cost recovery by using it as a road salt or other uses where extreme purity is not required.

Acknowledgements

Eastern Shore Microbes (ESM) is now introducing its proprietary biologically based sustainable *Halophilic Evaporative Applications Technology (H.E.A.T.)* process for use in the industry. The authors thank Mr. Charles Hall of MSC Engineering in Virginia Beach, Virginia for production of the CAD tables used in this work. They also are indebted to Dr. Anthony Nicastro for assistance verifying calculations, volumes and surface area data of the lagoons.

Statement of Financial Interest

The authors declare that they are owners of Eastern Shore Microbes and as such maintain a financial interest in the H.E.A.T. process.

References

1. Baas-Becking, L.G.M.; Historical Notes on Salt and Salt-Manufacture. *Scientific Monthly*, 31, 434 – 446, 1931.
2. Litchfield, C.D.L., Irby, A. and Vreeland, R.H.; The Microbial Ecology of Solar Salt Plants. *In:* Oren, A. Microbiology and Biogeochemistry of Hypersaline Environments, pp 39 – 52, 1998.
3. Obianyo, J.I.; Effect of Salinity on Evaporation and the Water Cycle. *Emerging Science Journal*, 3, 255 – 262, 2019.
4. Vreeland, R.H., Mierau, B.D., Litchfield C.D. and Martin E.L.; Relationship of the internal solute composition to the salt tolerance of Halomonas elongata. *Can. J. Microbiol*. 29, 407-4l4 1983.
5. Delzer, G.C. and McKenzie, S.W. 5 Day Biochemical Oxygen Demand, USGS TWRI Book 9 3rd ed, A7 pp21, 2003.
6. BIOCHEMICAL OXYGEN DEMAND (BOD) 5210B, *Standard Methods for the Examination of Water and Wastewater* DOI: 10.2105/SMWW.2882.102; 2021
7. Heiri, O. Lotter, A. and Lemcke, G.; Loss on ignition as a method for estimating organic and carbonate sediments: reproducibility and comparability of results, *Journal of Paleolimnology*, 25, 101-110, 2001.
8. https://wrcc.dri.edu/Climate/comp_table_show.php?stype=pan_evap_avg

Retanning Performance of Carboxymethyl Starch and Its Effects on Dyeing

by
Cigdem Kilicarislan Ozkan[1] and Hasan Ozgunay[1*]
[1]*Faculty of Engineering, Department of Leather Engineering, Ege University*, 35100 Bornova, Izmir, Turkey

Abstract

The tanning characteristics of starch samples modified by different methods were investigated in our previous studies. In this study, utilization of modified starch in leather making as a retanning agent and its effect on dyeing process have been investigated. For this purpose, the molecular size of native corn starch was reduced by H_2O_2 oxidation and then carboxymethylated. A series of analyses (water solubility, degree of substitution, Fourier Transform Infrared Spectroscopy, Proton and Carbon Nuclear Magnetic Resonance Spectroscopy) were carried out for characterization. Then, carboxymethyl starches were used in retanning processes to be 3, 5 and 10% based on leather weight and the shrinkage temperatures and filling coefficients of the leathers were determined. Acid and metal complex dyestuffs were used in dyeing processes and the effect of carboxymethyl starch on dyeing was also investigated by examining dye consumption, dry and wet rubbing fastness and color of the leathers. From the results it was concluded that carboxymethyl starch showed a noticeable solo performance in terms of filling property and shrinking temperature without any considerable adverse effect on dyeing.

Introduction

In recent years, the increasing awareness regarding the environment and human health, and the legal restrictions that have come into force in parallel, have significantly affected and put pressure on the leather industry as well as many other industries. This situation has made it necessary to replace existing production technologies and chemicals with more environmentally friendly technologies and chemicals. For this reason, many researchers have focused on the production of alternative chemicals from natural, renewable resources and the development of more environmentally friendly production methods. In fact, considering these consumer demands and trends for production, the sustainability of many products' production seems to depend on these studies. Because, whether the products are natural or not, their effects on the environment and human health are becoming more and more decisive in the purchasing behavior of consumers.

In line with these considerations, we focused on the usability of starch obtained from natural and renewable resources, which is used as a raw material in many industries,[1] in the leather industry by changing its structure with different modification methods. In our previous studies,[2-4] we tried to determine the tanning properties by modifying starch with different methods. In this study, the performance of carboxymethyl starch in retanning, whose tanning efficiency was previously investigated, was examined. As it is known, almost any substance with tanning properties can be used in retanning process. However, the possible negative effects of these tanning agents, especially on dyeing and color, may limit their use in retanning in some cases. For this reason, this issue was especially taken into consideration within the scope of the research and the effects of carboxymethyl starch on dyestuff consumption, color and fastness properties were investigated as well as the retanning efficiency of it.

Materials and Methods

Materials

Native corn starch was used as raw material and purchased from Hasal Starch Company Izmir/Turkey. Hydrogen peroxide (H_2O_2, 34.5-36.5%), copper (II) sulphate pentahydrate ($CuSO_4.5H_2O$, 99-100.5%), ethanol (C_2H_6O, 99.8%), hydrochloric acid (HCl, 37%), acetone (C_3H_6O, 99.5%), methanol (CH_3OH, ≥99.7%), silver nitrate ($AgNO_3$, 99.5%), sodium hydroxide (NaOH, 98-100.5%), hydroxylamine hydrochloride (NH_2OH*HCl, ≥98%), sulfuric acid (H_2SO_4, 95-97%) and monochloro acetic acid ($C_2H_3ClO_2$, 99%) were used in starch modifications and analyzes. All chemicals were purchased from Sigma Aldrich. Wet-blue goat leathers were used in retanning experiments.

Methods

Hydrogen Peroxide (H_2O_2) Oxidation of Native Corn Starch

Oxidation process of native corn starch was carried out as described by Zhang et al..[5] First of all, 10 grams of dehumidified starch was weighed and dispersed in 100 mL of distilled water. This mixture was stirred moderately with a magnetic stirrer at 80°C for 30 minutes. After that the temperature was reduced to 55°C and 0.1% $CuSO_4.5H_2O$ (dissolved in enough water) was added to the mixture and stirred again for 30 minutes. Then H_2O_2 was added and stirred another 30 minutes. In oxidation processes, the starch and H_2O_2 molar ratio was taken to be 1:10 considering the data from our previous study[2] in which it was determined that oxidized starch

*Corresponding author email: hasan.ozgunay@ege.edu.tr
Manuscript received August 24, 2021, accepted for publication September 27, 2021.

Figure 1. Oxidized starch: after dry in oven **(a)** and after grind **(b)**

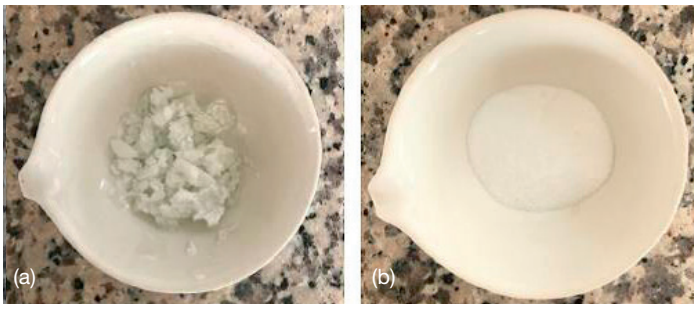

Figure 2. Carboxymethylated starch: after dry in oven **(a)** and after grind **(b)**

products with a molecular weight of 2737-2897 Da can be obtained by 1:10 molar ratio (starch:hydrogen peroxide) that can easily penetrate between leather fibers. $CuSO_4$ and H_2O_2 were calculated according to glucose units of starch molecules. After completion of the reaction, firstly the oxidized starch was precipitated in excess of ethanol and then centrifuged. The product was dried in an oven at 50°C for 48 hours. Finally, the dried product was ground.

Then, the obtained powder oxidized starch samples were subjected to carboxymethylation. For this reason, oxidation and carboxymethylation processes were repeated a few times until adequate amount was achieved to be used in retanning processes.

Determination of Product Yields

The yield of H_2O_2 oxidized starch was determined according to the method described by Kilicarislan Ozkan et al..[2] The experiments were performed in three repetitions and the yield of H_2O_2 oxidation was calculated by Formula (1) given below.

$$\% \text{ Yield} = \frac{\text{Obtained oxidized starch (g)}}{\text{Amount of native starch used (g)}} \times 100 \qquad \text{(Formula 1)}$$

Determination of carboxyl and carbonyl contents of H_2O_2 oxidized starch

The carboxyl and carbonyl contents of oxidized starch were determined according to the methods described by Chattopadhyay et al.[6,7] and Smith et al.[7,8] respectively. The experiments were performed with three replications and the results were given as mean data. Carboxyl and carbonyl contents were calculated according to Formula 2 and Formula 3, respectively.

$$DO_{COOH} = \frac{162C(V_1 - V_2)}{1000W - 36C(V_1 - V_0)} \qquad \text{(Formula 2)}$$

Where; C=NaOH solution concentration (mol/L), V_0=Volume of NaOH used for blank (mL), V_1=Volume of NaOH used for sample (mL), W=Dry weight of sample.

$$DO_{CO} = \frac{C(V_0 - V_1) \times (36DO_{COOH} + 162)}{1000W} \qquad \text{(Formula 3)}$$

Where; C=HCl solution concentration (mol/L), V_0=Volume of HCl used for blank (mL), V_1=Volume of HCl used for sample (mL), W=Dry weight of sample.

Carboxymethylation of H_2O_2 oxidized starch

Carboxymethylation process was also applied to the H_2O_2 oxidized starch samples. Carboxymethylation was performed by the method described by Hebeish et al.[9] with slight modification.[4] First of all, 8.1 g oxidized starch, 9.45 g monochloroasetic acid, 10 mL of 5 N NaOH solution and 45 mL distilled water were added in a 100 mL flask. Oxidized starch:Monochloroacetic acid:NaOH molar ratios were taken to be 1:2:1. The mixture was stirred to obtain a homogenous mixture. Then, the flask was transferred into the water bath at 50°C and shaken for 1 hour. After that, the flask was removed from the water bath and the reaction products were precipitated with ethanol. Then it was washed with ethanol until the alkalis were removed. The obtained product was dried in an oven at 50°C for 48 hours and then ground to get powder form.

The yields were calculated according to the Formula 1, where *obtained carboxymethyl starch* value was used in numerator and *amount of oxidized starch* value was used in denominator.

Determination of degree of substitutions

The degree of substitution (DS) of carboxymethylated starch (CMS) was determined according to the titrimetric method described by Jiang et al.[10] The DS was determined by using Formula 4 and Formula 5.

$$DS = \frac{n_{NaOH} \times M_o}{m_c - n_{NaOH} \times M_R} \qquad \text{(Formula 4)}$$

$$m_c = m_p - \left[\frac{mp \times F}{100}\right] \qquad \text{(Formula 5)}$$

Where; M_o=the molar mass of anhydroglucose unit (162 g/mol), M_R=the molar mass of carboxymethyl residue (58 g/mol), n_{NaOH}=the quantity of sodium hydroxide used (mol), m_p=the weight of polymer taken (g), m_c=the corrected weight of polymer (g), F=the moisture (%).

Determination of Water Solubility of Starches

The water solubility of native, H_2O_2 oxidized and carboxymethylated starch samples were investigated to determine the extent of changes in water solubility with modifications. Water solubility was

determined according to the method described by Singh and Singh[11] with slight modification[2-4] and Formula 6 was used for calculation.

$$\text{Water solubility \%} = \frac{\text{Supernatant solid weight (g)} \times 2}{\text{Sample weight (g)}} \times 100 \quad \text{(Formula 6)}$$

Structure Characterizations

The changes in the structures of native, oxidized and carboxymethylated starches by modifications were identified by FT-IR, ^{1}H-NMR and ^{13}C-NMR analyses. The FT-IR spectra were recorded in the range of 4000-650 cm^{-1} by Perkin Elmer Spectrum 100 FT-IR spectrometer. The ^{1}H-NMR and ^{13}C-NMR spectra were gained on a MERCURYplus-AS 400 MHz spectrometer (Ege University, NMR Satellite Laboratory, Izmir/Turkey). DMSO-d6 was used as solvent.

The Use of Carboxymethyl Starch in Retanning Process

In order to carry out the retanning trials with best possible homogenous materials; neck, flank and belly parts of the wet-blue goat leathers were removed and 30×30 cm size of pieces were cut from the remaining croupon part and used in retanning processes. The obtained carboxymethyl starches were used in retanning processes to be 3, 5 and 10% based on the chrome tanned leather weight. After retanning processes the leather samples were dyed with 3% of acid (Acid Blue 25) and metal complex (Acid Blue 360) dyestuffs, in order to investigate dyeing properties with alternative dyeing agents. The process recipe is given in Table I. Additionally, for each dyestuff, 2 samples were also processed according to the same recipe without carboxymethyl starch introduction to be used as blank samples.

Table I

Retanning and dyeing recipe

PROCESS	AMOUNT (%)	PRODUCT	TEMP. (°C)	TIME (min.)	pH
Washing	200	Water	40		
	0,2	Cationic Wetting Agent		15	
Draining					
Washing	100	Water	25	5	
Draining					
Neutralization	200	Water	38		
	2	Neutralizing Syntan		10	
	0,25	$NaHCO_3$		20	
Washing	100	Water	35	5	6.0
Draining					
Retanning	50	Water	37		
	x	CMS		45	
	3	Dyestuff		45	
	2	Phosphoester based fatliquor	50		
	5	Sulphite Natural+synthetic fatliquor combination			
	2	Synthetic fatliquor with high light fastness		45	
Fixing	0,8	HCOOH		20	
	0,7	HCOOH		30	3,5
Draining					
Washing	100	Water	25	10	
Draining					

Post-Retanning Tests

- **Determination of filling coefficient**
  The changes in leather thickness after retanning process were determined according to the TS EN ISO 2589[12] standard. Before retanning (T_1) (after neutralization) and after retanning (after fixation) (T_2) the thicknesses of the leathers were measured in wet form by using thickness gauge with 100 g pressure and the filling coefficients were calculated according to Formula 7.

$$\text{Filling coefficient (\%)} = \frac{T_2 - T_1}{T_1} \times 100 \qquad \text{(Formula 7)}$$

- **Determination of shrinkage temperature**
  The shrinkage temperatures (T_s) of the leather samples retanned with different ratios of carboxymethyl starches were measured according to ISO 3380[13], in order to determine possible effect on hydrothermal stability of the leathers.

- **Dyestuff consumption**
  Since retanning agents may alter the reactivity between leather and dyestuff, the amounts of dyestuffs remaining at the end of dyeing processes were measured by using Shimadzu UV-1601 spectrophotometer, so as to investigate probable favorable or unfavorable effect of carboxymethyl starch retanning on dye consumption.

- **Wet and dry rubbing fastnesses**
  The wet and dry rubbing fastnesses of dyed leathers were determined according to TS EN ISO 11640[14] standard test method and the evaluation was done according to the Grey Scale Standard (ISO 105-A02[15] and ISO 105-A03[16]).

- **Determination of color changes**
  Minolta CM-2600d spherical spectrophotometer with CIE 100 standard observer angle and CIE standard D65 daylight source was used to measure the colors and to evaluate the color differences of the leathers. The colors of all leather samples and differences compared with the control sample were evaluated according to the CIELAB color coordinate system.

Results and Discussion

Moisture contents of starches

The moisture contents of native corn starch and oxidized starch were found to be 9.7% and 7.2%, respectively. Since the ratio of starch to reagents used in oxidation and carboxymethylation processes is an important parameter, the moisture contents of native and oxidized starches were taken into consideration and pre-dehumidified starches (in an oven at 50°C for 48 h) were used in modifications.

Product yields, DS and water solubilities of starches

The product yields, degree of substitutions and water solubilities of oxidized and carboxymethylated starches were comparatively given in Figure 3.

From the evaluation of the data regarding the yields of oxidized and carboxymethylated starches, it was observed that the yield of carboxymethyl starch is lower than oxidized starch. Correspondingly, it was concluded that the carboxymethyl groups included in the structure of oxidized starch by the carboxymethylation process increased the water solubility of oxidized starch and consequently the obtained yield value decreased. Indeed, the higher water solubility value of carboxymethylated starch compared to its oxidized form (Figure 3) supports this idea.

The intra-granular structure of starch becomes irregular by oxidative degradation and introducing carboxymethyl groups therefore the water can easily enter to amorphous regions along with disruption of intramolecular hydrogen bonds.[17] As a matter of fact, comparing with the water solubility of native starch (0.9%), it can be seen that the solubility of native starch increased significantly with oxidation. However, it was observed that the solubility of the oxidized starch, which has already good water solubility, increased a bit more by introducing carboxymethyl groups into the structure with carboxymethylation process. During hydrogen peroxide oxidation, hydroxyl groups in C-2, C-3 and C-6 of glucose units can be replaced by carbonyl and carboxyl groups. Although the primary group introducing into the starch structure by H_2O_2 oxidation is carbonyl

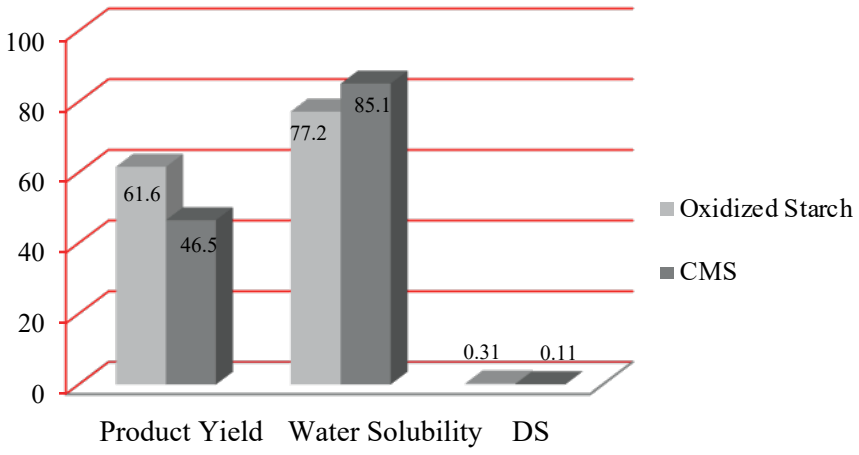

Figure 3. The product yields, degree of substitutions and water solubilities of oxidized and carboxymethyl starches

groups, a small amount of carboxyl groups are also included into the structure. The value 0.31 in Figure 3 shows the substituted carbonyl groups, however, the carboxyl groups included into the structure was determined to be 0.02. These results confirmed that carbonyl is the primary functional group produced in peroxide oxidized starches, although small amounts of carboxyl groups also formed. Throughout the first period of the reaction time in hydrogen peroxide oxidation, too much reagent is consumed for hydrogen removal during the formation of high amounts of carbonyl groups, less oxidant remains for the oxidation of carbonyl to carboxyl groups, for this reason the primary group formed by hydrogen peroxide oxidation is carbonyl group.[18]

Comparing degree of substitutions, it was determined that the degree of substitution from carboxymethylation is lower than oxidation. Which means the number of carboxymethyl groups introduced into the structure was determined to be less than the number of carbonyl groups. The underlying reason is that many of the hydroxyl groups having substitution ability in C-2, C-3 and C-6 in starch molecule have already been replaced mostly with carbonyl and smaller amounts of carboxyl groups by pre-applied oxidation process, therefore a few hydroxyl groups remained in oxidized starch molecule to substitute with carboxymethyl groups. Indeed, Hebeish et al.[9] similarly remarked that the carbonyl and carboxyl groups which included to structure by oxidation cause a decrease in carboxymethylation efficiency. Regarding the degree of substitution, it should be noted that starches with lower degree of substitution are obtained when water is used as the reaction medium in the carboxymethylation process. Spychaj et al.[19] also stated that when the carboxymethylation of native starch is carried out by using water, the degree of substitution can be achieved up to 0.07.

Structure Characterizations

The FT-IR spectra of native, oxidized and carboxymethyl starches were shown in Figure 4. As it is seen, although all starch samples have a very similar structure, some minor changes in the spectra of modified starches show that modification processes (oxidation and carboxymethylation) were carried out effectively. Comparing with the spectrum of native corn starch, a new absorption band at 1733.02 cm^{-1} was seen in spectrum of oxidized starches and it is assigned to C=O stretching vibration.[5,20-22] This peak indicates the addition of carbonyl and/or carboxyl groups to the native starch structure.

From examining the CMS spectrum, the new peak occurred at 1731.57 cm^{-1}, distinct from native starch, belongs to C=O stretching vibrations. Although this peak was also previously seen in the FT-IR spectra of oxidized starches with H_2O_2 at 1733.02 cm^{-1}, it was noticed that it was more pronounced in carboxymethylated derivatives. This is an evidence for including additional carboxyl groups into the structure because the protonated carboxylic groups (-COOH) similarly give the C=O band at 1733.02 cm^{-1}.[23,24] In addition, the peaks at 1603.18 and 1234.34 cm^{-1} which are attributed to characteristic carboxylate (-COO-) absorption peaks of carboxymethyl starch[10,24] became more prominent and OH absorption peak of native starch at 1358.21 cm^{-1} decreased with carboxymethylation.[25] The obtained FT-IR spectra proved that the carboxymethylation process applied to hydrogen peroxide oxidized starches was successfully carried out.

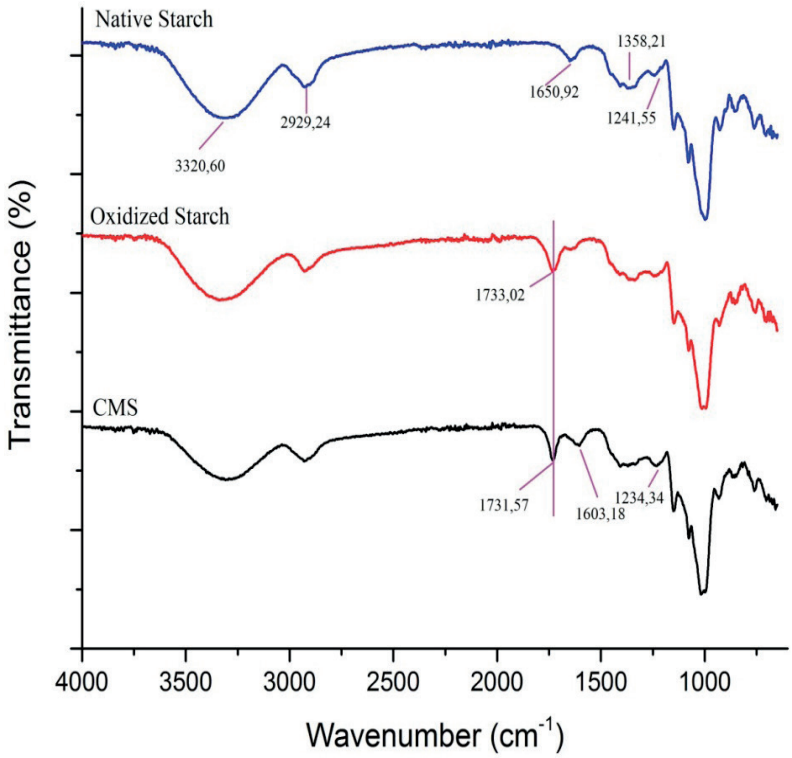

Figure 4. FT-IR spectra of native, oxidized and carboxymethylated starches

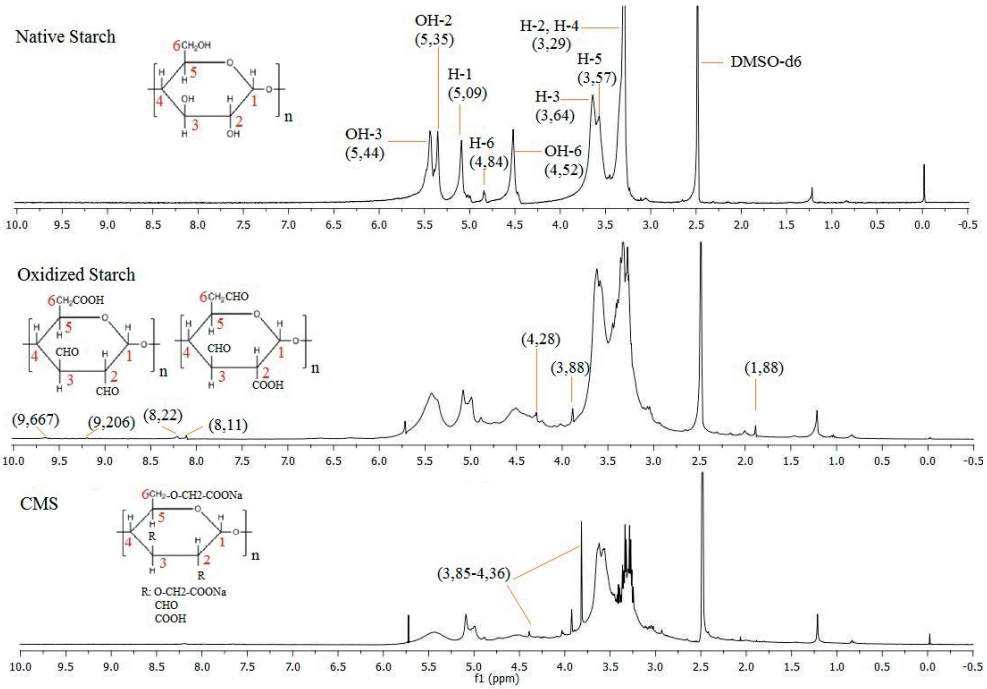

Figure 5. [1]H-NMR spectra of native, oxidized and carboxymethylated starches

Native starch, oxidized starch and CMS were also analyzed by NMR in order to see more clearly the changes occurred in chemical structure by oxidation and carboxymethylation processes. The [1]H-NMR spectra of starches were shown in Figure 5. Firstly, [1]H-NMR spectrum of native corn starch was inspected in order to identify the changes occurred in structure by modifications and some characteristic peaks were indicated in the native starch spectrum.

Comparing the [1]H-NMR spectra of native and oxidized starches, it was observed that the intensity of peaks, which indicate the proton signals of OH groups in C-2, C-3 and C-6 of native corn starch, decreased significantly with oxidation which indicates that the hydroxyl groups at C-2, C-3 and C-6 of glucose units substituted to some extent. On the other hand, the observed changes in the spectrum of native corn starch in H-1 (5.09 ppm) and H-6 (4.84 ppm) proton signals at the α→1.4 and α→1.6 junctions confirmed that these bonds were broken down during oxidation. Unlike native starch, the small signals seen around 9.21-9.67 ppm in the spectrum of oxidized starch are ascribe to protons of carbonyl groups (aldehydic group),[26,27] the new signals at 8.11-8.22 ppm and 3.88-4.28 ppm are attributed to the protons of –OH and –CH groups of hemiacetal structures.[27]

From the [1]H-NMR spectrum of CMS (Figure 5), the new signals occurred between 3.85-4.36 ppm, differently from oxidized starch, showed that carboxymethylation process is effective on oxidized starches. However, OH-6 proton signal (4.52 ppm) which was seen in the spectrum of oxidized starch disappeared in the carboxymethylated starch that indicates that the carboxymethylation preferably takes place on C-6. On the other hand, comparing with the spectra of oxidized starch, the loss of the signal at 1.88 ppm which is attributed to the protons of the CH_2 group next to the carbonyl or carboxyl group in oxidized starch also confirmed that the carboxymethyl groups mostly replaced with the group in C-6. In addition, the changes seen in the OH-2 and OH-3 signals in the spectrum of oxidized starches after carboxymethylation showed that the substitution also actualized in these groups.

[13]C-NMR spectra of native, oxidized and carboxymethyl (CMS) starches were shown in Figure 6. The signals seen at 60.87, 71.99-73.63, 79.15 and 100.47 ppm in [13]C-NMR spectrum of native starch are attributed to the C-6, C-2, C-3, C-5, C-4 and C-1 carbons, respectively.[28] Comparing with the [13]C-NMR spectrum of native starch, the intensity of C-1 peak decreased and two peaks (102.51 and 99.14 ppm) appeared here because of the carboxymethylation status of C-2. In this respect, two different situations could occur for C-1, depending on if there is carboxymethyl substitution of C-2 or not. These peaks suggested that the carboxymethyl substitution at C-2 causes a shift ~ 1 ppm on C-1.[29] Differently from native starch; the signals seen at 163.48 and 174.84 ppm in the spectrum of oxidized starch are attributed to carbonic and carboxylic carbons, respectively.[28] As seen in the spectra of oxidized starch, the peak of CHO group is slightly clear than the peak of COOH group it confirms that the primary group introducing into the structure in peroxide oxidation is carbonyl group. In addition, the intensity of C-2 and C-4 signals significantly decreased in comparison to the native starch spectrum. This decline in signal levels may arise from starch depolymerization mainly in α-(1→4)-glucosidic linkages.[30]

However, the intensity of C-2, C-3 and C-6 signals in native starch spectrum significantly decreased by oxidation, it is shown that OH groups at C-2, C-3 and C-6 of glucose units replaced with CHO and COOH groups.[28] Differently from [13]C-NMR spectra of native and oxidized starches, the peak clearly seen at 180.42 ppm is attributed to the -CO carbon of carboxymethyl group and proves

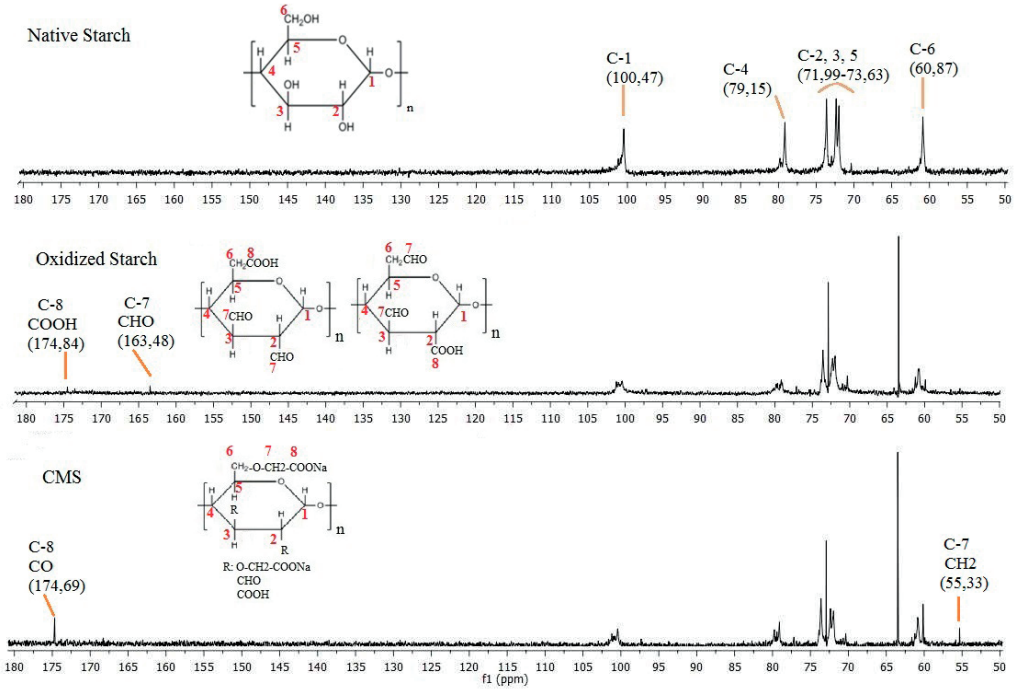

Figure 6. ^{13}C-NMR spectra of native, oxidized and carboxymethylated starches

that the carboxymethylation process is carried out effectively. In addition, it is seen that the signal of C-1 in oxidized starch spectrum does not change remarkable in CMS spectrum. It confirms that carboxymethylation mostly takes place in the C-6 position.[29]

Retanning and dyeing experiments

Hydrothermal stability and filling coefficient test results of the leathers retanned with 3, 5 and 10% of CMS were given in Table II. From the evaluation of the results, it was seen that the thicknesses and shrinkage temperatures of the leathers increased for all CMS treated samples in conjunction with increasing amount used in retanning. However, the maximum increments in shrinkage temperature and filling coefficient were determined to be 5-6 °C and 6.3-7.1%, respectively with 10% CMS ratio which can be regarded as a noticeable solo performance for retanning.

Table II

The results of hydrothermal stability and filling coefficient gained to the wet-blue goat leathers

The Group Dyed with Acid Dyestuff		
CMS amount used in retanning	**Filling coefficient (%)**	**Shrinkage temperature (°C)**
(Control Sample)	0.7	109
3%	3.5	112
5%	4.4	113
10%	6.3	115
The Group Dyed with Metal-Complex Dyestuff		
CMS amount used in retanning	**Filling coefficient (%)**	**Shrinkage temperature (°C)**
(Control Sample)	0.9	109
3%	4.6	111
5%	6.4	112
10%	7.1	114

Consumption of Dyestuff

The amounts of dyestuffs remaining in the bath at the end of the dyeing processes are given in Table III. From the evaluation of the results, although a noticeable increase (amount of dyestuff remaining in the bath) was detected especially for the 10% of CMS retanned sample comparing with blank sample, in general considering the amounts of dyestuffs remaining in the baths (especially 3 and 5% of CMS introductions) it is possible to say that dye consumption values after CMS retannage are in acceptable limits and does not have drastic negative effect on it.

Wet and dry rubbing fastness of dyed leather samples

Dry and wet rubbing fastness tests were applied to the CMS retanned and dyed leather samples in order to investigate possible effect of CMS retannage on dyed crust leathers' fastness properties.

Table III

The amounts of dyestuffs remaining in dyeing baths (g/L)

CMS amount used in retanning	**Acid Blue 25 (Acid Dyestuff)**	**Acid Blue 360 (Metal-Complex Dyestuff)**
	Start conc. 60	Start conc. 60
Control sample	0.009	0.010
3%	0.022	0.019
5%	0.025	0.024
10%	0.036	0.071

Table IV

Wet and dry rubbing fastness results of dyed leather samples

		Dry Rubbing		Wet Rubbing	
		Acid Dyestuff	Metal-Complex Dyestuff	Acid Dyestuff	Metal-Complex Dyestuff
Control	Leather	4/5	4/5	3/4	3/4
	Felt	4	4	2	4
3% CMS	Leather	3/4	4/5	4	3/4
	Felt	4	4	2/3	4
5% CMS	Leather	4	4/5	4	4
	Felt	4/5	4	2/3	4/5
10% CMS	Leather	4	4/5	4/5	4/5
	Felt	4/5	4	2	4/5

The test results were given in Table IV. From the evaluation of the results it was seen that use of CMS as retanning agent did not result in a remarkable effect on leathers' crust fastness properties. This also means that CMS retannage did not cause accumulation of dye on leather surface. However, predictably dying with metal-complex dyestuff resulted in better fastness properties comparing to dying with acid dyestuff especially for wet-rubbing tests.

Color Differences

Another important issue on retannage and dying is retanning agents' possible effect on color and shade depending on their structure and color. So as to determine any effect on color/shade, the colors of the CMS retanned leathers were measured and also compared with the control sample. The color measurements and comparisons with control sample data were given in Table V.

From the examination of the data (Table V), it was determined that the color slightly shifted towards green compared to the control sample in conjunction with increasing amount of CMS in leathers dyed with acid dyestuff which cannot be perceived with naked eye. However, in metal-complex dyed leathers, although any alteration in shade was not detected, a significant alteration was detected in L value which means the color intensity of leathers increased by CMS introduction in retannage.

Conclusion

The molecular size of native corn starch ($2.227x10^6$ Da) which is too large to penetrate between leather fibers was reduced by H_2O_2 oxidation (between 2737-2897 Da) then oxidized starch was also carboxymethylated. A series of analysis (water solubility, degree of substitution, FT-IR, ^{1}H-NMR, ^{13}C-NMR) were carried out for characterization and to investigate the structural changes by modifications. The results obtained from analysis confirmed that the modifications were successfully carried out. Considering the test and analysis results of the retanning performance of carboxymethyl starch, it was concluded that it showed a remarkable retanning effect in terms of filling property and shrinking temperature increment without any considerable adverse effect on dyestuff consumption, color fastness and color properties, which are also should be taken in account in performance evaluation of a retanning agent.

Table V

Color measurement values of leathers retanned with CMS at different ratios and dyed afterwards

The Group Dyed with Acid Dyestuff							
Sample	**L**	**a**	**b**	**dL**	**Da**	**db**	**dE**
Control	33.71	0.49	-35.62				
3% CMS	34.39	-0.50	-34.08	0.68	0.99	1.54	1.95
5% CMS	35.38	-0.86	-37.01	1.67	1.35	1.39	2.56
10% CMS	34.23	-1.19	-35.51	0.52	1.68	0.11	1.76
The Group Dyed with Metal-Complex Dyestuff							
Sample	**L**	**A**	**b**	**dL**	**Da**	**db**	**dE**
Control	36.14	-1.24	-17.73				
3% CMS	33.09	-1.11	-17.36	3.05	0.13	0.37	3.08
5% CMS	34.53	-1.06	-17.18	1.61	0.18	0.55	1.71
10% CMS	32.25	-0.72	-16.63	3.89	0.52	1.10	4.08

Where: L: lightness / brightness (L=0 black, L=100 white), a: red/green color (+a red, -a green), b: yellow/blue color (+b yellow, -b blue) and dL, da, db and dE the changes in color compared to the control sample.

Acknowledgements

We would like to thank the Ege University Faculty of Engineering Scientific Research Projects Commission, which supported this study financially (Project No: 18MUH004).

References

1. Averous, L.; Biodegradable multiphase systems based on plasticized starch: A review, *Journal of Macromolecular Science, Part C: Polymer Reviews* 44, 231-274, 2004.
2. Kilicarislan Ozkan, C., Ozgunay, H. and Akat, H.; Possible use of corn starch as tanning agent in leather industry: Controlled (gradual) degradation by H_2O_2, *International Journal of Biological Macromolecules* 122, 610-618, 2019. https://doi.org/10.1016/j.ijbiomac.2018.10.217
3. Kilicarislan Ozkan, C. and Ozgunay, H.; Alternative Tanning Agent for Leather Industry from a Sustainable Source: Dialdehyde Starch by Periodate Oxidation, *Journal of the American Leather Chemists Association* 116(3), 89-99, 2021.
4. Kilicarislan Ozkan, C. and Ozgunay, H.; Production of Carboxymethyl Starches from Oxidized Starches and Determination of Their Tanning Characteristics, *Journal of the American Leather Chemists Association* 116(6), 187-197, 2021.
5. Zhang, Y.R., Wang, X.L., Zhao G.M. and Wang, Y.Z.; Preparation and properties of oxidized starch with high degree of oxidation, *Carbohydrate Polymers* 87(4), 2554–2562, 2012. https://doi.org/10.1016/j.carbpol.2011.11.036
6. Chattopadhyay, S., Singhal, R.S. and Kulkarni, P.R.; Optimisation of conditions of synthesis of oxidized starch from corn and amaranth for use in film-forming applications, *Carbohydrate Polymers* 34(4), 203–212, 1997. https://doi.org/10.1016/S0144-8617(97)87306-7
7. Yi, X., Zhang, S. and Ju, B.; Preparation of water-soluble oxidized starch with high carbonyl content by sodium hypochlorite, *Starch-Stärke* 65, 1–9, 2013. https://doi.org/10.1002/star.201300037
8. Smith, R., Whistler, R. and Paschall, E.; Starch Chemistry and Technology, Academic Press, New York, 1967.
9. Hebeish, A., Khalil, M. I. and Hashem, A.; Carboxymethylation of starch and oxidized starches, *Starch/Stärke* 42(5), 185-191, 1990. https://doi.org/10.1002/star.19900420506
10. Jiang, Q., Gao, W. Li, X. Liu, Z. Huang, L. and Xiao, P.; Synthesis and properties of carboxymethyl Pueraria thomsonii Benth, *Starch/Stärke* 63, 692-699, 2011. https://doi.org/10.1002/star.201100047
11. Singh, J. and Singh, N.; Studies on the morphological and rheological properties of granular cold water soluble corn and potato starches, *Food Hydrocolloids* 17(1), 63-72, 2003. https://doi.org/10.1016/S0268-005X(02)00036-X
12. TS EN ISO 2589, Leather - Physical and Mechanical Tests - Determination of Thickness, 2016.
13. ISO 3380, (IULTCS)/IUP 16), Leather-Physical and mechanical tests-Determination of shrinkage temperature up to 100°C, 2015.
14. TS EN ISO 11640, Leather- Tests for colour fastness- Colour fastness to cycles of to-and-fro rubbing, 2018.
15. ISO 105-A02, Textiles - Tests for colour fastness - Part A02: Grey scale for assessing change in colour, 1993.
16. ISO 105-A03, Textiles - Tests for colour fastness - Part A03: Grey scale for assessing staining, 2019.
17. Chong, W., Uthumporn, U., Karim, A. and Cheng, L.; The influence of ultrasound on the degree of oxidation of hypochlorite-oxidized corn starch, *LWT- Food Science and Technology* 50, 439-443, 2013. https://doi.org/10.1016/j.lwt.2012.08.024
18. Sangseethong, K., Termvejsayanona, N. and Sriroth, K.; Characterization of physicochemical properties of hypochlorite- and peroxide-oxidized cassava starches, *Carbohydrate Polymers* 82, 446-453, 2010. https://doi.org/10.1016/j.carbpol.2010.5.003
19. Spychaj, T., Wilpiszewska, K. and Zdanowicz, M.; Medium and high substituted carboxymethyl starch: Synthesis, characterization and application, *Starch/Stärke* 65, 22-33, 2013. https://doi.org/10.1002/star.201200159
20. Kweon, D., Choi, J., Kim, E. and Lim, S.; Adsorption of divalent metal ions by succinylated and oxidized corn starches, *Carbohydrate Polymers* 46(2), 171–177, 2001. https://doi.org/10.1016/S0144-8617(00)00300-3
21. Para, A.; Complexation of metal ions with dioxime of dialdehyde starch, *Carbohydrate Polymers* 57(3), 277–283, 2004. https://doi.org/10.1016/j.carbpol.2004.05.005
22. Hui, R., Qi-he, C., Ming-liang, F., Qiong, X. and Guo-qing, H.; Preparation and properties of octenyl succinic anhydride modified potato starch, *Food Chemistry* 114(1), 81–86, 2009. https://doi.org/10.1016/j.foodchem.2008.09.019
23. Wang, Y., Gao, W. and Li, X.; Carboxymethyl Chinese yam starch: Synthesis, characterization, and influence of reaction parameters, *Carbohydrate Research* 344, 1764-1769, 2009. https://doi.org/10.1016/j.carres.2009.06.014
24. Spychaj, T., Wilpiszewska, K. and Zdanowicz, M.; Medium and high substituted carboxymethyl starch: Synthesis, characterization and application, *Starch/Stärke* 65, 22-33, 2013. https://doi.org/10.1002/star.201200159
25. Lu, S.H., Liang, G.Z., Ren, H.J., Wang, J.L. and Yang, Q.R.; Synthesis and application of graft copolymer retannage of degraded starch and vinyl monomers, *Journal of the Society of Leather Technologies and Chemists*, 89(2), 63-66, 2005.
26. Malafaya, P.B., Elvira, C., Gallardo, A., San Román, J. and Reis, R.L.; Porous starch-based drug delivery systems processed by a microwave route, *Journal of Biomaterials Science, Polymer Edition*, 12(11), 1227-1241, 2001. https://doi.org/10.1163/156856201753395761
27. Ye, Y., Ren, H., Zhu, S., Tan, H., Li, X., Li, D. and Mu, C.; Synthesis of oxidized β-cyclodextrin with high aqueous solubility and broad-spectrum antimicrobial activity, *Carbohydrate Polymers* 177, 97-104, 2017. https://doi.org/10.1016/j.carbpol.2017.08.123
28. Ye, S., Qiu-hua, W., Xue-Chun, X., Wen-yong, J., Shu-Cai, G. and Hai-Feng, Z.; Oxidation of cornstarch using oxygen as oxidant without catalyst, *Food Science and Technology* 44, 139-144, 2011. https://doi.org/10.1016/j.lwt.2010.05.004
29. Lawal O.S., Lechner M.D., Hartmann B. and Kulicke W.M.; Carboxymethyl Cocoyam Starch: Synthesis, Characterisation and Influence of Reaction Parameters, *Starch/Stärke* 59, 224-233, 2007. https://doi.org/10.1002/star.200600594
30. Yu, Y., Wang, Y., Ding, W., Zhou, J. and Shi, B.; Preparation of highly-oxidized starch using hydrogen peroxide and its application as a novel ligand for zirconium tanning of leather, *Carbohydrate Polymers* 174, 823-829, 2017. https://doi.org/10.1016/j.carbpol.2017.06.114

Lifelines

Md. Abdur Razzaq is working as a Scientific Officer in Leather Research Institute, Bangladesh Council of Scientific and Industrial Research (BCSIR), Nayarhat, Savar, Dhaka-1350, Bangladesh. He completed his BSc. (Hons.) degree in Leather Engineering from Institute of Leather Engineering and Technology, University of Dhaka, Bangladesh and MS degree in Applied Chemistry and Chemical Technology from Islamic University, Kushtia, Bangladesh. His research interests are: leather processing, chemical and environmental research.

Murshid Jaman Chowdhury is working as a Senior Scientific Officer in Leather Research Institute, Bangladesh Council of Scientific and Industrial Research (BCSIR), Nayarhat, Savar, Dhaka-1350, Bangladesh. He did BSc. (Hons.) and MS degree from the department of Applied Chemistry and Chemical Engineering, University of Dhaka, Bangladesh. His research interests are: leather processing, chemical and environmental research.

Md. Tushar Uddin is working as a Senior Scientific Officer in Leather Research Institute, Bangladesh Council of Scientific and Industrial Research (BCSIR), Nayarhat, Savar, Dhaka-1350, Bangladesh. He completed PhD degree from the department of Chemistry, Jahangirnagar University, Bangladesh. He also did my BSc. (Hons.) and MSc. degree from the department of Applied Chemistry and Chemical Technology, University of Rajshahi, Bangladesh. His research interests are: leather processing, chemical and environmental research.

S. Vasanth is an Assistant Professor in the Department of Mechatronics Engineering at the School of Mechanical Engineering Kattankulathur Campus, SRM Institute of Science and Technology Chennai, Tamilnadu, India. He is pursuing Doctor of Philosophy(Ph.D) in the area of power diode based laser beam machining under mechatronics faculty in SRM IST, Chennai. He received Master of Engineering (M.E) in Mechatronics at Madras Institute of Technology, Anna University, Chennai in 2012. Research interests include: laser materials processing, control systems and mechatronics.

T. Muthuramalingam, Associate Professor, Department of Mechatronics Engineering, School of Mechanical Engineering, Kattankulathur Campus, SRM Institute of Science and Technology, Chennai, Tamilnadu, India. He received his Ph.D in Mechanical Engineering from Mechanical Madras Institute of Technology, Anna University in 2013. In 2008 he earned a Master's degree in Mechatronics from Madras Institute of Technology, Anna University. His research interests include unconventional micro machining, manufacturing automation, process optimization and design of experiments and energy conservation.

Sanjeev Gupta, see *JALCA* **108**, 156, 1998

Russell Vreeland received his microbiological training at Rutgers University (BS and MS), the University of Nebraska-Lincoln (PhD) and Post-Doctoral training at University of Western Ontario. He was a Professor at the University of New Orleans and at West Chester University of Pennsylvania. He is a chauvinist about two things: microorganisms and pollinators of all types. As a microbiologist he knows that it is really microbes that run the Earth while the rest of us often just mess it up. His initial training focused on marine microbiology during which he became fascinated by the microbes that live and function in extremely high salts and their potential application for industry. He focused entirely on the marvelous microbes that survive and thrive in saline waters anywhere from 2× to 10× the concentration of seawater and even in salt crystals. He also led teams studying the remains of the ancient oceans (large underground salt deposits) as a geological microbiologist where he reanimated the world's oldest living microbes (120 and 250 million years old) and the world's oldest known DNA sequences (412 MYA). He is the founder, President and Chief Scientist for Eastern Shore Microbes (ESM).

John Long became a partner in Eastern Shore Microbes in 2018. Mr. Long graduated from Northampton High School and Johnson and Wales University with an Associate's Degree in Culinary Arts and an emphasis in marketing and management. As the ESM chief of logistics and operations Mr. Long applies all of the experience gained from a career in farming, corporate production, shipping and quality control. His primary corporate emphasis focuses on maintaining the highest levels of quality standards, ingredients and nutrient production procedures to always exceed ESM's and client's expectations. His responsibilities include warehousing nutrient supplies, mixing nutrient formulations for all lagoons, shipping and equipment maintenance for ESM.

Cigdem Kilicarislan Ozkan graduated from Ege University Department of Leather Engineering in 2008. The same year she started to M.Sc. She studied on extraction of vegetable tanning materials. She joined the staff of Leather Engineering Department as research assistant in 2010 and completed her PhD in 2018. Her research activities and fields of interests are: tanning materials, extraction techniques, modification of biopolymers and leather technologies.

Hasan Ozgunay studied Leather Technology at the University of Ege (Turkey). After working in Leather Industry for one year, he joined the staff of Leather Engineering Department as research assistant in 1996. He obtained his M.Sc. in the same department. He studied on vegetable tanning materials and obtained his PhD in Leather Engineering. He is currently working as researcher / lecturer in the Leather Engineering Department. His research activities and fields of interests are: tanning materials, leather processing technologies and cleaner leather processing methodologies.

LEATHER

AVELLISYNCO

Selected Dyestuffs

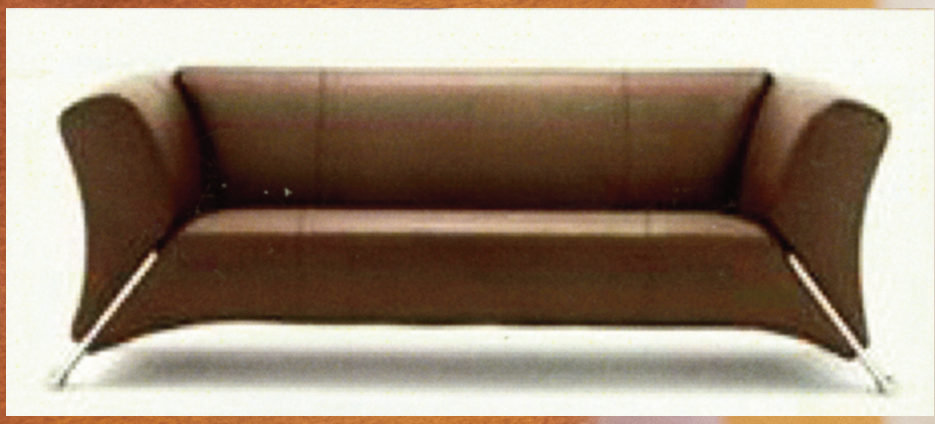

CHEMTAN

17 Noble Farm Drive • Lee, NH 03861 (Office)
57 Hampton Road • Exeter, NH 03833 (Manufacturing)
Tel: (603) 772-3741 • Fax: (603) 772-0796
www.CHEMTAN.com

Obituary

Martin Heise passed away on December 9 after a long battle against cancer.

Martin began his leather career in 1986 upon completion of the leather technician course at Lederinstitut Gerberschule Reutlingen (LGR). In a long professional career spanning 35 years, he worked for Sudleder, two tanneries namely Bayern-Leder-GmbH (BLG), Naturin, and TFL. He then worked for Trumpler for more than twenty years and finally with Royal Smit & Zoon as Head of Produce Management for wet-end leather chemicals since 2019.

Speaking on behalf of the VGCT Board, Dr Dietrich Tegtmeyer of TFL said the following: "On December 9 our colleague, friend and buddy Martin passed away after a long illness. We got to know and appreciate him as someone who was an inspiring, convincing ambassador for leather as well as a highly professional advisor for many of us. We will all miss him very much."

In 1994 he joined the VGCT and since 2014 he was a board member. In 2016 he was appointed Chairman. For his dedication to the leather industry, he was honored with the 2021 VGCT annual award for lifetime achievement. This was awarded by the VGCT to express their appreciation for his constant commitment to leather, the needs of the tanning industry and the people who work in it. The training of apprentices and prospective technicians was a particular interest for him.

Martin was a member of The American Leather Chemists Association since May of 2004 and regularly attended many of our Annual Conventions.

Martin was a popular figure both in his native Germany as well as the global tanning industry. He was a kind and courteous person and was always fun to be around. He was a strong advocate for leather and the leather industry and regularly posted or shared positive stories on social media.

INDEX TO ADVERTISERS

CALL FOR PAPERS

FOR THE 116th ANNUAL CONVENTION OF THE AMERICAN LEATHER CHEMISTS ASSOCIATION

Eaglewood Resort & Spa, Itasca, Illinois
June 21-24, 2022

If you have recently completed or will shortly be completing research studies relevant to hide preservation, hide and leather defects, leather manufacturing technology, new product development, tannery equipment development, leather properties and specifications, tannery environmental management, or other related subjects, you are encouraged to present the results of this research at the next annual convention of the Association to be held at the Eaglewood Resort & Spa, Itasca, Illinois, June 21-24, 2022.

Abstracts are due by April 1, 2022
Full Presentations are due by June 1, 2022

They are to be submitted by e-mail to the
ALCA Vice-President and Chair of the Technical Program:

Joseph Hoefler
The Dow Chemical Company
400 Arcola Rd.
Collegeville, PA 19426
E-mail: jhoefler@dow.com

The **Abstract** should begin with the title in capital letters, followed by the authors' names. An asterisk should denote the name of the speaker, and contact information should be provided that includes an e-mail address. The abstract should be no longer than 300 English words, and in the Microsoft Word format.

Full Presentations at the convention will be limited to 25 minutes. In accordance with the Association Bylaws, all presentations are considered for publication by *The Journal of the American Leather Chemists Association.* They are not to be published elsewhere, other than in abstract form, without permission of the *Journal* Editor. For further paper preparation guidelines please refer to the *JALCA* Publication Policy on our website: leatherchemists.org

Full Presentations are to be submitted by e-mail to the *JALCA* editor:

Steven D. Lange, *Journal* Editor
The American Leather Chemists Association
E-mail: jalcaeditor@gmail.com
Mobile Phone (814) 414-5689

116th ALCA ANNUAL CONVENTION June 21-24, 2022 Eaglewood Resort & Spa Itasca, IL

Featuring the 61st John Arthur Wilson Memorial Lecture

"Road Ahead"

By Randy Johnson, President and CEO

PANGEA

Formerly GST Seton

Tentative Schedule

Tuesday, June 21

Golf Tournament, Opening Reception and Dinner

Wednesday, June 22

John Arthur Wilson Memorial Lecture
All Day Technical Sessions, Fun Run
Reception and Dinner, Activities - Bowling, Pool, Darts and an Open Bar

Thursday, June 23

All Day Technical Sessions, Annual Business Meeting
Activities Awards Luncheon
Social Hour, ALCA Awards Banquet

Visit us at www.leatherchemists.org for full details under Annual Convention as they become available

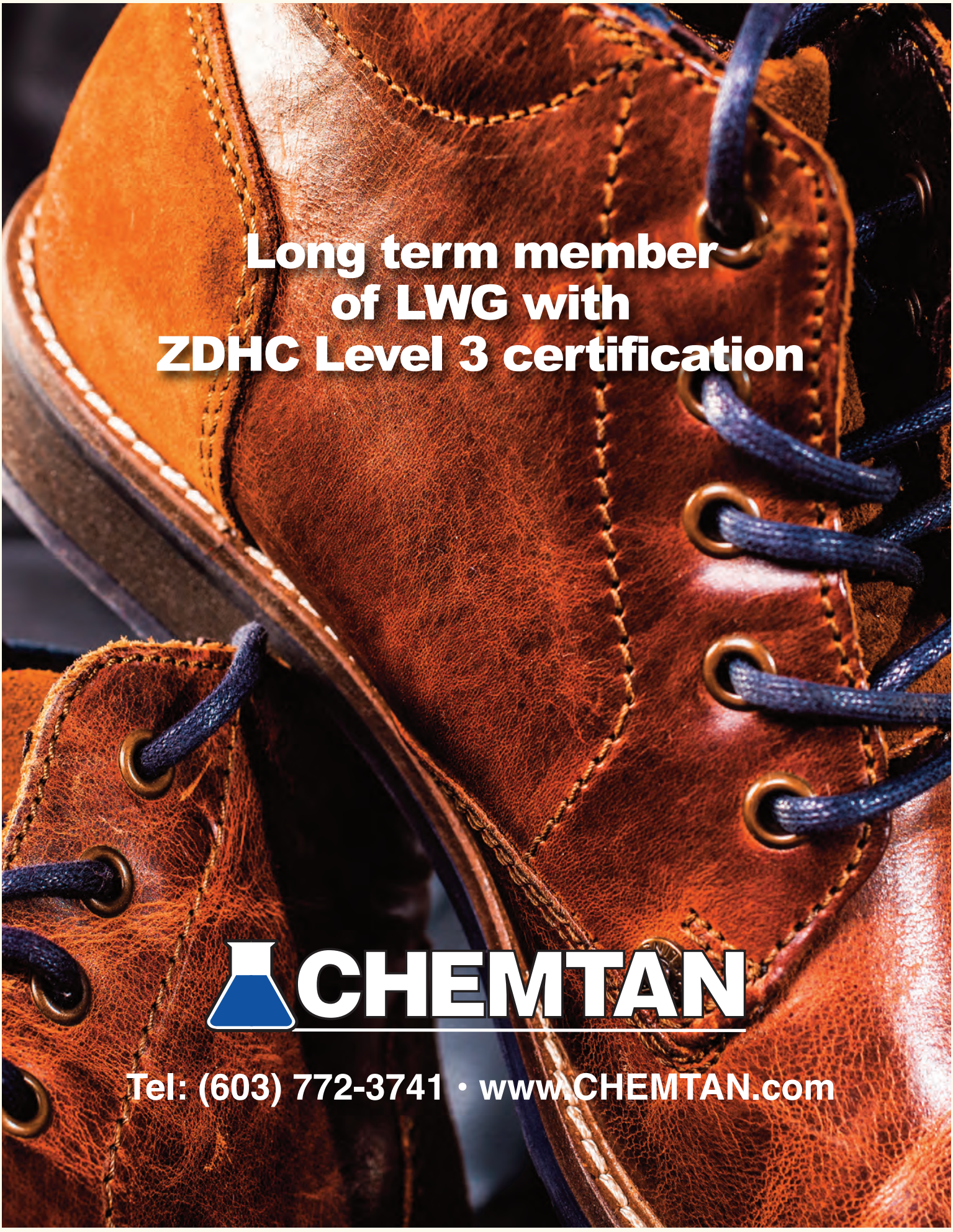
Long term member
of LWG with
ZDHC Level 3 certification
CHEMTAN
Tel: (603) 772-3741 • www.CHEMTAN.com